

RM A53H03

NACA RM A53H03

**CASE FILE
COPY**



RESEARCH MEMORANDUM

AN ANALYTICAL STUDY OF THE COMPARATIVE PERFORMANCE
OF SIX AIR-INDUCTION SYSTEMS FOR TURBOJET-
POWERED AIRPLANES DESIGNED TO OPERATE
AT MACH NUMBERS UP TO 2.0

By Earl C. Watson

Ames Aeronautical Laboratory
Moffett Field, Calif.

**NATIONAL ADVISORY COMMITTEE
FOR AERONAUTICS
WASHINGTON**

October 9, 1953
Declassified August 16, 1957

NACA RM A53H03

NATIONAL ADVISORY COMMITTEE FOR AERONAUTICS

RESEARCH MEMORANDUM

AN ANALYTICAL STUDY OF THE COMPARATIVE PERFORMANCE
OF SIX AIR-INDUCTION SYSTEMS FOR TURBOJET-
POWERED AIRPLANES DESIGNED TO OPERATE
AT MACH NUMBERS UP TO 2.0

By Earl C. Watson

SUMMARY

The study reported in NACA RM A52C14 considered the problems of inlet design and performance for Mach numbers up to 1.5. Extension of that study to Mach numbers of 2.0 is presented in the present report. A two-dimensional inviscid analysis is used to compare the performance of several types of inlets when used in conjunction with a turbojet engine having constant-volume air flow. The performance was evaluated on the basis of a summation of drag factors which included additive drag, air-bypass drag, and thrust loss resulting from a loss of total pressure. Of these factors the latter is the most significant, especially at the higher Mach numbers. Additive drag may become large for some off-design operating conditions. The necessity for using an air-bypass system with most inlet designs is indicated. For inlets having the same assumed pressure recovery, substantial improvements in inlet-engine matching over an operating range of Mach numbers from 0.85 to 2.0 occurred with those inlets having variable geometry. The variations of entrance area and diffuser contraction required for ideal inlet-engine matching throughout the range of Mach numbers are indicated.

INTRODUCTION

An analytical study of various types of inlets for an air-induction system for a turbojet-powered airplane intended to operate at Mach numbers from 0.85 to 1.5 at an altitude of 35,332 feet (the lower limit of the stratosphere) was presented in reference 1. Air-induction systems having divergent diffusers, with fixed and variable inlet areas, and with and without external ramps were investigated. The four inlet types considered were compared on the basis of a drag evaluation which accounted

for the thrust loss accompanying a total-pressure loss, for additive drag, and for the drag resulting from bypassing excess air. It was shown that the thrust loss associated with a loss of total pressure is the most important of these factors. It was concluded that variation of inlet area should not be necessary for Mach numbers up to 1.5, provided the system with fixed inlet area is equipped with an internal air-bypass system.

The purpose of the study considered herein is to predict the operational characteristics of inlets similar to those discussed in reference 1 but intended for operation at Mach numbers from 0.85 to 2.0 and at altitudes from sea level to the stratosphere. The inlets with external ramps were modified from those studied in reference 1 to suit the design requirements at a Mach number of 2.0. Two additional inlet configurations are included in this report. One is a fixed-geometry type of inlet with an external ramp and a convergent-divergent diffuser. The other is a variable-geometry type with a variable convergent-divergent diffuser and with a variable inlet area.

The method of analysis relates the engine and inlet air-flow characteristics to free-stream conditions and is valid for either two- or three-dimensional flow. Although only two-dimensional-inlet flow conditions were considered in the analysis, and although the results are limited to two-dimensional inlets, the study delineates important factors which must be considered in the design of inlets intended to operate at Mach numbers up to 2.0. The limiting Mach number of 2.0 was selected for this investigation primarily because at this Mach number high ram-compression ratios and temperature ratios occur which may be detrimental to the operation of turbojet engines of current designs (ref. 2).

NOTATION

The following notation is used in this report:

a	speed of sound, ft/sec
A	area, sq ft
A ₀	cross-sectional area of the free-stream tube of air admitted by the inlet, sq ft
A _{0R}	cross-sectional area of the free-stream tube of air required by the engine, sq ft
A _r	reference area for drag factors (assumed to be 1 sq ft)
C _p	static-pressure coefficient, $\frac{p-p_0}{q_0}$

F_n	net thrust of a turbojet engine, lb
$F_{n_{100}}$	net thrust of a turbojet engine for $\frac{H_3}{H_0} = 1.0$, lb
g	acceleration due to gravity, ft/sec ²
H	total pressure, lb/sq ft
K_{Da}	additive-drag factor, $\frac{1}{A_r} \int_S C_{p_s} dA_x$
K_{DH}	thrust-loss factor resulting from the total-pressure loss $\frac{H_3}{H_0}, \frac{F_{n_{100}} - F_n}{q_0 A_r}$
K_{DW}	drag factor corresponding to the thrust loss accompanying an air-bypass process, $\frac{m}{A_r q_0} (V_0 - \eta V_j)$
ΣK_D	summation of drag factors, $K_{DH} + K_{DW} + K_{Da}$
m	mass-flow rate of air, slugs/sec
M	Mach number
N	percent of rated engine rotational speed
p	static pressure, lb/sq ft
q	dynamic pressure, lb/sq ft
t	static temperature, °R
T	total temperature, °R
V	velocity, ft/sec
V_j	theoretical jet-exit velocity of bypassed air, ft/sec
w_a	weight rate of air flow, lb/sec
w_{ac}	corrected weight rate of air flow, $w_a \frac{\sqrt{\theta'}}{\delta'}$, lb/sec
δ	ramp angle, deg
δ'	pressure correction for the weight rate of air flow, $\frac{H_3}{P_{s1}}$
θ	the wave angle of an oblique shock wave, deg
θ'	temperature correction for the weight rate of air flow, $\frac{T_3}{T_{s1}}$

- ρ mass density of air, slugs/cu ft
- η nozzle exit velocity coefficient, the ratio of the actual exit velocity to the theoretical exit velocity of the bypassed air (assumed to be 0.97)

Subscripts

- e entrance of the inlet, considered to be at the leading edge of the lip and perpendicular to the direction of the entering flow
- m minimum area of a convergent-divergent diffuser
- o free stream
- s stream tube bounding the air entering the inlet
- sl standard ambient conditions at sea level
- x projection in the direction of the free-stream flow of the stream tube bounding the air entering the inlet
- 1, 2 stations immediately behind a shock wave (fig. 1)
- 3 entrance to the compressor of the engine, station 3
- l lip

DESCRIPTION OF THE INLETS

The nomenclature used in the analysis is shown in figure 1 for an air-induction system having a scoop-type inlet with an external ramp. That portion of the air-induction system near the entrance is considered to be the inlet, and station 3 corresponds with the exit of the diffuser (the entrance to the compressor of the engine). A sketch and basic description of each of the inlets is shown in figure 2. Three types with fixed inlet area are shown. Of these, inlet A corresponds in type, but not in geometric detail, to inlet A of reference 1 and inlet C is the same as inlet C of reference 1. Inlet E represents a third type with a fixed inlet area. It has a fixed external ramp, different from the ramp of inlet A, and it has a convergent-divergent diffuser. Inlets B and D have a variable geometry and correspond in type but not in

geometric detail with inlets B and D, respectively, of reference 1. Inlet F is a variable-geometry type which combines the convergent-divergent-diffuser feature of inlet E, and the variable-inlet-area feature of inlet D.

ASSUMPTIONS

When the air flow between the free stream and the exit of the diffuser was considered, it was assumed that the continuity relationship applies to the flow and that the total temperature is constant. With these two assumptions the flow could be either two or three dimensional. Because the shock-wave patterns for inlets in three-dimensional flow are more complex than those in two-dimensional flow, the performance analysis of the inlets is based on two-dimensional-flow theory and utilizes the charts and tables of reference 3 in conjunction with the shock-wave patterns shown for each inlet shown in figure 3. Abrupt transition from one shock-wave pattern to another was assumed. For the inlets with external ramps to produce oblique shock waves, a normal shock wave was assumed to occur at the leading edge of the ramp for Mach numbers below that for which an oblique shock wave would detach from the ramp. Sharp lips were assumed for the inlets so that there would be no detached shock waves caused by the lips. For inlets with divergent diffusers it was assumed that supersonic flow could enter the inlet and that a normal shock wave would occur just inside the entrance at a Mach number equal to that at the entrance. The surfaces immediately ahead of the inlets or ramps were assumed to be aligned with the free-stream flow; the effects of the boundary layer and of the forebody were not considered. Variations of pressure drag of the external surfaces of the inlets with changing flow conditions also were not considered.

Figure 4 shows the variation of total-pressure ratio H_3/H_0 with free-stream Mach number assumed for the air-induction system with each of the inlets. The potential pressure recovery of each system is limited by the shock-wave configurations at the inlet. Included in figure 4 for comparative purposes are the theoretical total-pressure ratios which would result from isentropic compression from the supersonic free stream and the best theoretical total-pressure ratio which could result from a compression of the flow by means of one oblique and one normal shock wave (best two-shock recovery). For Mach numbers between 0.85 and 1.5 the variation of total-pressure ratio with Mach number for inlets A, B, C, and D was the same as that given in reference 1 for the corresponding type of inlet. As in reference 1, for Mach numbers above 1.31 the total-pressure ratio for inlets C and D was assumed to be 95 percent of the total-pressure ratio across a normal shock wave occurring at the free-stream Mach number; the pressure recovery assumed for inlets A, B, E, and F was based on results from an accumulation of published data for various types of inlets.

The assumed characteristics of the turbojet engine used for the analysis were the same as those of reference 1 but were extended to a flight Mach number of 2.0. Figure 5(a) shows the corrected weight of air flow as a function of corrected rotational speed for the engine. Since the engine was assumed to be operating at rated rpm ($N=100$ percent), the corrected air flow is also shown as a function of the temperature correction factor. The assumed net thrust of the engine is shown in figure 5(b) for operation at rated speed, with afterburning, for an altitude of 35,332 feet, and for various total-pressure ratios.

OPERATIONAL CHARACTERISTICS OF THE ENGINE AND THE INLETS

In the following paragraphs the assumed flow conditions for the engine and the inlets are discussed in detail, and further consideration is given to the geometric characteristics of each inlet. As indicated in references 4 and 5, the air-flow requirements of the engine in terms of free-stream-tube area provide an indication of the entrance-area requirements for the inlet. In this report the air-flow requirements of the engine and the air-flow delivery of the inlets are expressed as the free-stream-tube areas A_{OR} and A_O , respectively, and equations are presented for calculating each of these areas. Equations are given, also, for the calculation of the drag factors used to evaluate the relative performances of the inlets (i.e., additive drag, air-bypass drag, and thrust loss resulting from a loss of pressure recovery).

Air Requirements of the Engine

The corrected weight of air flow required by the engine and the free-stream-tube area A_{OR} can be related using the definition of corrected weight of air flow

$$w_{ac} = w_a \frac{\sqrt{\theta'}}{\delta'} = \frac{w_a \sqrt{(T_3/t_0)(t_0/T_{s1})}}{(H_3/H_0)(H_0/p_0)(p_0/p_{s1})}$$

where $w_a = g \rho_0 A_{OR} V_0$ ($A_{OR} = A_O$ for perfect matching)

Hence,

$$A_{OR} = \frac{w_{ac} (H_3/H_0) (\theta')^3}{g \rho_{s1} a_{s1} (t_0/T_{s1})^3 M_0} \quad (1)$$

The temperature correction factor θ' as a function of Mach number and altitude is shown in figure 6. The variations of A_{OR} with Mach number for altitudes from sea level to 35,332 feet (see fig. 7) were

calculated from equation (1) utilizing the corrected weight rate of air flow for the assumed engine from figure 5(a) and the assumed total-pressure recoveries from figure 4. Because of the isothermal nature of the stratosphere, A_{OR} for any altitude in the stratosphere will be the same as A_{OR} calculated for an altitude of 35,332 feet. For Mach numbers above approximately 1.3 the divergence of the curves for the various pressure recoveries indicates the large effect that pressure recovery has on A_{OR} (fig. 7). Obviously, the large variation of A_{OR} required by the engine for operation over a wide range of Mach number and altitude - even for poor pressure recovery - presents a considerable problem to the designer of inlets.

In Appendix A equations are developed, with general design assumptions, for the air-flow characteristics of a turbojet engine. If an essentially constant-volume type of operation is assumed, and if the mass flow is proportional to the stagnation density at the compressor, then equation (A5) indicates that A_{OR} has a specific variation with Mach number for a constant altitude.

Comparison of the variation of A_{OR} with Mach number for isentropic pressure recovery for the assumed engine (fig. 7) with that given by equation (A5) of Appendix A indicates that the variations are essentially the same. It is apparent from the development of the equations that the general design problems and operational characteristics of the inlets discussed in this report apply to a general type of turbojet engine; that is, to that of essentially constant-volume operation (engine speed equal to rated rpm). For other types of engine operation, such as with variable rpm, with water injection, etc., the air-flow requirements of the engine would differ from those of this study, and, consequently, the design problems and operational characteristics of the inlets would be modified. It is beyond the scope of this report to consider other types of engine operation.

Flow Conditions, Designs, and Air Delivery for the Inlets

General flow considerations.- The continuity equation used in conjunction with the definition of mass-flow ratio relates the flow conditions in the inlet to the flow conditions in the free stream. This relationship is

$$\frac{A_O}{A_e} = \frac{m_e}{m_O} = \frac{H_e (1+0.2M_O^2)^3 M_e}{H_O (1+0.2M_e^2)^3 M_O} \quad (2)$$

for a ratio of specific heats for air of 1.4. Equation (2) can be applied to either two- or three-dimensional steady flow when appropriate values are used for the terms. When A_O/A_e has been found by use of this

equation (which is independent of altitude) then the area in the free stream through which the air flows prior to entry into the inlet, A_0 , can be calculated provided A_e is known. When shock waves exist in the flow and if the diffuser is convergent-divergent instead of divergent, the form of equation (2) may be modified to apply to the appropriate conditions. Figure 8 shows the modified forms of the equation which apply to the particular two-dimensional-flow conditions and shock-wave configurations assumed in the analysis. (See fig. 3 for the shock-wave configurations for each inlet.)

Inlet A.- Inlet A is a fixed-geometry type having an external ramp followed by a divergent diffuser. The entrance area A_e is 1.48 square feet in order to admit the amount of air required by the engine for the low-speed design condition at a mass-flow ratio of 1.0 ($M_0 = 0.85$; alt. = 35,332 ft; $A_{OR} = 1.48$ (fig. 7)). The ramp angle was selected to provide the highest pressure recovery for the largest range of flight Mach numbers. At a given Mach number there is a range of ramp angles for which the pressure recovery varies only slightly from its optimum two-shock value. Therefore, there is some freedom in the selection of the value for the ramp angle for an inlet. In figure 9 two ranges of values for the ramp angle are indicated. For ramp angles within one range the pressure recovery across an oblique and a normal shock wave occurring at a given Mach number would be between the best two-shock value and 0.995 times the best two-shock value. In the other range the pressure recovery would be between the best two-shock value and 0.990 times the best two-shock value for a given Mach number. A ramp angle of 12° was selected for inlet A since the pressure recovery for an oblique and normal-shock-wave combination (see fig. 3 for inlet A for $M_0 > 1.5$) is equal to, or greater than, 99 percent of the best two-shock pressure recovery for a wide range of Mach numbers (fig. 9). The conditions that the diffuser is divergent, that the entrance area has a specific value, and that the shock wave from the external ramp at a Mach number of 2.0 must intersect the leading edge of the lip (for additive drag to be zero) determine the position of the sharp lip with respect to the ramp.

When an oblique shock wave is attached to the ramp, the wave angle θ is dependent on the free-stream Mach number M_0 and the ramp angle δ (the relationship can be obtained from the charts and tables of ref. 3). The mass-flow ratio A_0/A_1 is a function of the wave angle θ and ramp angle δ . Because of the interdependence of the Mach number, wave angle, ramp angle, and mass-flow ratio, if any two are known, or assumed, the others can be calculated or ascertained from charts or figures based on the interrelationship. In this analysis it was found that a graph of θ versus δ for constant M_0 and A_0/A_1 was convenient.

With the shock wave attached to the ramp of inlet A (for $1.5 \leq M_0 \leq 2.0$), it was assumed that the stream tube entering the inlet would be parallel to the ramp, and that a normal shock wave would occur within, or at, the entrance of the inlet (station e). For these conditions equation (2d),

figure 8, can be simplified to show that A_0/A_e equals A_0/A_1 which can be determined for a given free-stream Mach number. With the shock wave detached from the ramp (for $M_0 \leq 1.5$, see fig. 3), the stream tube entering the inlet was also assumed to be parallel to the ramp so that the flow would enter the inlet at an average Mach number equal to the average Mach number existing after the detached (normal) shock wave. Equation (2b), figure 8, simplified for the divergent diffuser of inlet A, applies to the flow.

Figure 10(a) shows the variation with free-stream Mach number of the free-stream-tube area A_0 for the operating mass-flow ratios ($m_e/m_0 = A_0/A_e$) calculated for inlet A.

Inlet B.- The ramp angle of the external ramp of this type of inlet with variable geometry can be varied by rotating the ramp about a hinge at the leading edge of the ramp. For optimum two-shock pressure recovery the ramp angle must be varied with free-stream Mach number as shown in figure 9 for inlet B. The lip of the inlet is located so that the oblique shock wave from the ramp intersects the leading edge of the lip at a Mach number of 2.0. The entrance area is such that the free-stream area of the stream tube A_0 entering the inlet is the same as the area required by the engine ($A_0 = A_{0R}$). At lower Mach numbers excess air is admitted, because of the increase in the entrance area as the ramp angle is decreased, and it must be bypassed. Figure 3 shows that an oblique shock wave is attached to the ramp and that a normal shock wave is at the entrance for free-stream Mach numbers between 1.0 and 2.0. From figure 8 it can be seen that equation (2d), modified for a divergent diffuser, applies to the flow. Figure 10(b) shows the variation with free-stream Mach number of the mass-flow ratio and the free-stream-tube area A_0 for the operation of inlet B.

Several variations of the geometry of inlet B were investigated in an attempt to improve its performance. Instead of hinging the ramp, as indicated in figure 2, the ramp could slide with the ramp angle varying or remaining constant; also, the ramp could be hinged at the entrance to the inlet. Then, with a change of ramp angle different free-stream-tube areas of air would be admitted into the inlet. With either of these geometries no arrangement was devised that would always provide ramp angles in the range for good pressure recovery and, also, the proper amount of air. In the case with the ramp hinged at the entrance, the length of the ramp also must be variable for the oblique shock wave from the ramp to intersect the leading edge of the lip for all Mach numbers. With any of these variations for inlet B, best two-shock recovery is the optimum that can be expected, and operation without additive drag and excess air is difficult or impossible.

Inlet C.- For this inlet there is no external ramp, the diffuser is divergent, and the fixed area at the entrance is 1.48 square feet,

the same as that for inlet A. With a normal shock wave at, or within, the entrance the mass-flow ratio would always be 1.0, and the pressure recovery could be no greater than normal shock recovery. The total-pressure ratio H_3/H_0 assumed for this inlet is shown in figure 4. With the normal shock wave standing ahead of the entrance, which would occur for a wide range of Mach numbers if there were no air-bypass system, the mass-flow ratio would be less than 1.0 and air would spill around the entrance. The two types of operating conditions for inlet C are shown in figure 3. Equation (2b), figure 8, modified for a ramp angle equal to 0° , applies to the flow conditions for this inlet when the shock wave stands ahead of the entrance. The free-stream-tube area A_{OR} required by the engine for the pressure recovery of inlet C is shown in figure 7.

Figure 10(c) shows the variation of free-stream-tube area A_0 with free-stream Mach number for the operation of inlet C with the normal shock wave at the entrance ($A_0/A_e = 1.0$). Also shown in this figure are the mass-flow ratios required for operation of the inlet to deliver the proper amount of air with no air-bypass system.

Inlet D.- This inlet is similar to inlet C in that no external ramp is employed, but it differs in that the lip is hinged so that the inlet area can be varied. (See fig. 2.) As for inlets A and C, an entrance area of 1.48 square feet is required for operation at a Mach number of 0.85. The free-stream-tube area required for this inlet is the same as that for inlet C throughout the range of free-stream Mach numbers because the same variation of pressure recovery with Mach number was assumed. The value of A_{OR} does not exceed 1.48 square feet, the value of the entrance area for $M_0 = 0.85$ and a condition for which the diffuser is divergent (see fig. 7), and thus the diffuser always would be divergent for the range of Mach numbers considered. With the mass-flow ratio equal to 1.0 ($A_0/A_e = 1.0$), A_e equals A_{OR} so there would be no spillage at the entrance and the normal shock wave would always be at, or within, the entrance of the inlet (see fig. 3). Figure 10(d) shows the variation of free-stream-tube area A_0 with free-stream Mach number for operation of inlet D at a mass-flow ratio of 1.0.

Inlet E.- The factors influencing the design of a fixed-geometry inlet with a convergent-divergent diffuser are many, and they vary with the particular operational characteristics desired (i.e., contraction ratio, ramp angle, diffuser length, etc., must all be considered). The maximum contraction ratio, A_0/A_m , which permits the start of supersonic flow in the diffuser can be calculated by equation (2b), figure 8 (for $M_m = 1.0$ and $\delta = 0^\circ$). The contraction ratio required to compress isentropically a supersonic stream to a Mach number of 1.0 can be calculated by equation (2a), figure 8 (for $M_m = 1.0$ and $\delta = 0^\circ$). Figure 11 shows the variation of these contraction ratios with free-stream Mach number. Naturally, for any free-stream Mach number greater than 1.0,

the most favorable contraction ratio is the value for isentropic compression of the flow. However, because the value of the maximum contraction ratio which permits the start of supersonic flow is smaller, a compromise is necessary in choosing a value for the contraction ratio for an inlet designed to operate over a wide range of Mach numbers.

For inlet E the required area of the minimum section A_m was calculated by equation (2a), figure 8, with the assumption that $M_m = 1.0$, $M_o = 0.85$, and $A_o = A_{oR}$ for flight in the stratosphere at $M_o = 0.85$. Its value was found to be 1.45 square feet. An external ramp is employed so that with an oblique shock wave attached to the ramp at supersonic speeds the Mach number of the flow entering the inlet is less than the Mach number of the free stream. A value of 8° was selected for the ramp angle on the basis of two considerations. First, the combined total-pressure loss across the oblique shock wave from an 8° ramp, across the oblique shock wave from the inner surface of the lip, and across the normal shock wave near the minimum-area section was not considered excessive for free-stream Mach numbers up to 2.0. The second reason was involved with the interrelationship of the design of the lip, the Mach number behind the oblique shock wave from the ramp, and the contraction ratio to use for the inlet. For this inlet the contraction was provided by the inner surface of the lip and the ramp. The plane of the inner surface of the lip was located so that it made an angle of 4° with the entering flow. (See fig. 2.) The area at the entrance of the inlet, and, therewith, the location of the leading edge of the lip, were selected so that at a free-stream Mach number of 2.0 the shock wave from the external ramp would intersect the leading edge of the lip. This procedure resulted in a contraction ratio A_e/A_m of 1.095. For this contraction ratio supersonic flow cannot enter the inlet until the free-stream Mach number reaches about 1.79. Then the Mach number behind the oblique shock wave from the external ramp has a value for which a contraction ratio of 1.095 will permit the start of supersonic flow into the inlet.

Figure 3 shows the shock-wave configurations assumed for inlet E throughout the range of free-stream Mach numbers. For Mach numbers above 0.85 it was assumed that the inlet would be choked. When a shock wave was detached from the external ramp, the flow ahead of the inlet was considered in a manner similar to that for inlet A. When a shock wave was detached from the lip, the total-pressure ratio H_2/H_1 was assumed to be equal to the total-pressure ratio across a normal shock wave occurring at the Mach number M_1 . Equations (2a), (2b), (2c), and (2d), figure 8, apply, respectively, to the flow for the following ranges of free-stream Mach number: 0.85 to about 1.0, 1.0 to 1.34, 1.35 to 1.78, and 1.79 to 2.0. Figure 10(e) shows the variations of free-stream-tube area A_o and mass-flow ratio with free-stream Mach number for inlet E.

Inlet F.- This inlet was designed to obtain high pressure recovery throughout the range of Mach numbers. It combines the favorable

geometric characteristics of inlets E and D, namely, the convergent-divergent diffuser (variable for inlet F) and the variable inlet area. The lip is designed so that it can be rotated about a hinge, as in the case of inlet D, in order for A_o (or A_e) to equal A_{oR} throughout the ranges of Mach number and altitude. It is assumed that the floor of the inlet is flexible so that the contraction ratio A_e/A_m can be varied to permit supersonic flow to enter the inlet and to insure high pressure recovery.

Some idea of how the geometry of this type of inlet must vary can be obtained from consideration of the curve showing the variation of A_{oR} with free-stream Mach number and the curve showing the variation of A_o/A_m with free-stream Mach number for a Mach number of 1.0 at the minimum section. (See figs. 7 and 11, respectively, and consider an altitude of 35,332 ft.) From figure 7 it is apparent that A_{oR} is near a minimum for an M_o of about 1.2 and that for good pressure recovery A_{oR} increases as the free-stream Mach number is increased above, or decreased below, about 1.2. From figure 11 it can be seen that A_o/A_m is a minimum of 1.0 for $M_o = 1.0$ and that this contraction ratio increases as the free-stream Mach number increases above, or decreases below, 1.0. Thus, the position of the lip with respect to its hinge must vary so that A_e equals A_{oR} , and the contraction ratio A_e/A_m must be varied, first, in such a manner as to keep the normal shock wave inside the inlet; then, it can be increased to approach the value of A_o/A_m corresponding to that across the combined shock waves.

Figure 10(f) shows the variation of free-stream-tube area A_o with free-stream Mach number for the operation of inlet F for flight in the stratosphere. The area of the free-stream tube A_o would vary for operation at other altitudes in the same manner as A_{oR} (fig. 7), and the mass-flow ratio would always be 1.0 (fig. 10(f)). Further discussion of the design and operation of inlet F is presented in Appendix B.

Calculation of the Drag Factors

The loss of thrust resulting from a total-pressure-recovery ratio H_3/H_o of less than 1.0 was expressed, as in reference 1, in terms of the thrust-loss factor K_{DH} . The variations of this thrust-loss factor with free-stream Mach number for the inlets being considered are shown in figure 12. These results were calculated by use of the pressure recoveries shown in figure 4 and the engine performance shown in figure 5(b).

For joint operation of the engine and inlet, the difference between A_o and A_{oR} indicates that the proper amount of air would not be

delivered to the engine. Thus, for the inlets being considered, the excess air delivered to the engine is indicated by the difference between the area of the free-stream tube entering the inlet (A_O , from fig. 10) and the area of the free-stream tube required by the engine (A_{OR} , from fig. 7). The percentage of excess air based on the air delivery of the inlet is shown in figure 13 for each of the inlets. This excess air must be bypassed if the inlet and engine are to operate together at the assumed flow conditions. The drag factor K_{DW} was calculated, as indicated in reference 1, for each of the inlets in order to estimate the drag penalty involved with the air-bypass process. The drag factors resulting from bypassing the excess air are shown in figure 14 for each inlet for operation at 35,332 feet.

Methods for calculating the additive drag for inlets are given in references 6 and 7. As applied in this analysis, the solution of the drag equations is straightforward when there is no detached shock wave in the flow. When a detached shock wave exists, it may be detached from the lip or from the ramp, and the evaluation of the drag equations depends on the form and the location of the detached shock wave. With a shock wave detached from the lip the approximate method of reference 8 can be used for calculating the form and location of the detached shock wave. In order to calculate the additive drag with a shock wave detached from an external ramp (as for inlets A, B, and E), the form of the wave was assumed to be the same as that of a normal shock wave. The additive-drag factors are shown in figure 14 for the operation assumed for each inlet.

The summation of the drag factors accounting for the thrust loss associated with a loss of pressure recovery, the air-bypass drag, and the additive drag is defined by the equation

$$\Sigma K_D = K_{DH} + K_{DW} + K_{Da}$$

The variation of the summation of drag factors is shown in figure 15 for each of the inlets.

DISCUSSION AND COMPARISON OF THE INLETS

Air Delivery and Air Requirements

An evaluation of the relative performance of the inlets was made from the results of the preceding calculations. Combined in figure 16 are curves showing the variations with free-stream Mach number of A_O for each of the inlets (taken from fig. 10) and of A_{OR} for the engine (taken from fig. 7, for an altitude of 35,332 ft). It is evident from

figure 16 that only inlets D and F provide the proper amount of air to the engine throughout the speed range considered. Inlet B provides the proper amount of air only at the design Mach number ($M_0 = 2.0$); for all lower speeds the difference between A_0 and A_{0R} indicates that excess air is delivered by the inlet. Inlets A, C, and E deliver excess air throughout the speed range. (See fig. 13 for the percent of excess air delivered by each inlet.) Inlets A, B, C, and E, therefore, require an internal air-bypass system in order to operate at their calculated mass-flow ratios for the assumed flow conditions. Without air-bypass systems, excess air must be spilled around these inlets, and lower pressure recoveries and different flow conditions would have to be considered for a portion of the speed range. The operation of inlet C without an air-bypass system is considered in a following section.

Drag Factors

The air-bypass-drag factors accounting for the process of bypassing excess air are shown in figure 14 for each of the inlets. The curves indicate that the drag penalty of the air-bypass process is small for each of the inlets throughout the range of Mach numbers.

The penalty of additive drag is indicated by the additive-drag factor shown for each inlet in figure 14. Additive drag exists for inlets A, B, and E whenever the shock wave from the external ramp does not intersect the leading edge of the lip, and for inlet C when operating with air spillage around the inlet. The additional effect of reduced pressure recovery when operating with spillage was not considered. The additive-drag factor is maximum for inlet A at a free-stream Mach number of about 1.49 when the shock wave is detached from the external ramp. For inlet E the maximum additive-drag factor occurs at a free-stream Mach number of about 1.35 and the shock wave is also detached from the ramp. For most of the range of Mach numbers, the additive-drag factor for inlet B is smaller than for inlet A, or inlet E, because the ramp angle of inlet B is variable and the shock wave always is attached to the ramp. Two types of operation were considered for inlet C (see fig. 3) in order to compare the drag resulting from spillage of excess air. In the first case the normal shock wave is at or within the entrance of the inlet so that excess air must be bypassed, and in the other the normal shock wave is ahead of the entrance and air must be spilled around the inlet when no bypass is employed. It is evident from the drag factors shown in figure 14 that the drag penalty for the conditions assumed is less if excess air is bypassed rather than spilled. Experimental verification of the drag reductions possible with bypassing rather than spilling excess air is to be found in reference 9.

The effect of pressure recovery on inlet performance is indicated by the drag factor K_{DH} (fig. 12). For Mach numbers less than about 1.3

this drag factor is the same for each of the inlets because they have the same pressure recovery. For Mach numbers above 1.3 the curve for inlets C and D and the curve for inlets A, B, E, and F diverge, as would be expected from consideration of the pressure recoveries for the inlets (fig. 4).

The general effect of changes of altitude on the drag factors can be ascertained from consideration of the equation for each drag factor. It is evident from the equation for K_{DW} (see Notation) that at a given free-stream Mach number the air-bypass-drag factor depends on the amount of excess air to be bypassed. The variation of A_{OR} with Mach number is the same for all altitudes within the stratosphere but changes with lower altitudes, as shown in figure 7. The variation of A_O with Mach number is the same throughout the altitude range for inlets A, B, C, and E. At a given Mach number A_{OR} decreases as the altitude decreases below the stratosphere. Therefore, the percent of excess air and the air-bypass-drag factor both increase with decreasing altitude. The equation for K_{DA} (see Notation) indicates that at a given Mach number, the additive drag would remain constant with changes of altitude for the operating conditions of each inlet, provided air bypass is used. The variation of the thrust-loss factor with altitude is not readily apparent from the equation for K_{DH} (see Notation). However, for a given free-stream Mach number, if it is assumed that the ratio of $F_{n_{100}}$ at one altitude to $F_{n_{100}}$ at another altitude is proportional to the ratio of the air densities at the two altitudes, and since q_0 also would be proportional to the density, then the thrust-loss factor would change very little with changes of altitude.

Evaluation of Inlet Performance

The relative performance of the inlets was evaluated in this study by a summation of the drag factors. The variation of this summation with Mach number is shown in figure 15 for each of the inlets. At a given Mach number the inlet having the smallest drag summation is considered to have the best performance. It is evident from figure 15 that for the conditions considered, inlet F has the smallest drag summation throughout the range of Mach numbers and that the summation for inlet B is only slightly higher. Above a Mach number of about 1.5 inlets C and D are considerably worse than the other inlets; below a Mach number of 1.5 inlets A and E are considerably worse than the others. The interrelationship of the drag summations for the various inlets of reference 1 for the range of Mach numbers from 0.85 to 1.5 is similar to that shown in figure 15 for Mach numbers up to about 1.5.

Since the pressure recoveries for inlets A, B, E, and F are assumed to be the same, the difference between the drag summations for inlets A,

B, or E and that for inlet F at a given Mach number is the sum of the additive and air-bypass drag factors for the respective inlet. For inlet A the maximum difference (almost 60 percent) occurs at a Mach number of about 1.49 just before the detached shock wave attaches to the ramp. Likewise, at a Mach number of about 1.35 the maximum difference (53 percent) for inlet E occurs just before the detached shock wave attaches to the ramp. From figures 14(a) and 14(d) it can be realized that most of this difference between the drag summation for inlets A and E and that for inlet F results from the large increment of additive drag associated with the detached shock wave occurring with inlets A and E. Because the ramp of inlet B is varied so that no detached wave exists ahead of the inlet, the additive drag is small and the curve for the drag summation for inlet B has no peaks, such as occur in the curves for inlets A and E. Also for operation at 35,332-foot altitude the drag summation for inlet B is within 10 percent of that for inlet F which has no additive or air-bypass drag. However, at lower altitudes the difference would be greater. Thus, by comparing the curves for inlets A, B, and E, it is evident that detached shock waves in the flow ahead of an inlet are not desirable.

The summation of the drag factors for inlets C and D is high relative to those for the other inlets for Mach numbers greater than about 1.5, primarily, because of the low pressure recoveries of inlets C and D. This large influence of pressure recovery is apparent from a comparison of the summation of drag factors for inlets D and F which have no air-bypass drag or additive drag (figs. 15 and 14(e)), the only difference between the two curves being that due to pressure recovery. That pressure recovery becomes increasingly important as the Mach number is increased above 1.3 is indicated by the divergence of the curves for inlets D and F (fig. 15). At a free-stream Mach number of 2.0 the total-pressure ratio for inlet D was 0.14 less than that for inlet F (fig. 4). This increment of pressure recovery provided a drag summation for inlet D almost 80 percent greater than that for inlet F. The importance of obtaining high pressure recovery at high Mach numbers is evident.

In view of the large effects of pressure recovery on the over-all performance of the air-induction system, further consideration of the shock-wave configurations at the inlet is important. A single shock at the entry, such as is indicated for inlets C and D (fig. 3), limits the total pressure recovery available to normal shock recovery. With two or more shocks at the entry, such as for the other inlets, the pressure recovery available should be higher by an amount dependent upon the shock-wave patterns. It is therefore apparent that inlets having a geometry which provides multishock recovery at the entry to the air-induction system are most desirable for use in the range of Mach numbers considered here. With the design of inlet F, the geometry provides for the required variation of entrance area and diffuser contraction necessary for inlet operation supplying multishock pressure recovery without any penalty of additive drag, or the necessity for an air-bypass system.

Significance of the Drag Summation

The drag summation ΣK_D can be considered as a drag coefficient, within the limitations of the assumptions, if its value is divided by the proper reference area. To obtain some idea of the significance of this drag summation, it can be converted to drag-coefficient form based on wing area and compared with the drag coefficient of a hypothetical airplane. Assume an airplane, typical of those to fly in this Mach number range, having a wing area of 170 square feet and using 2 engines, each having the same characteristics as the engine assumed in this analysis. Then the drag summation in drag-coefficient form would be about 0.012 times the values shown in figure 15. At a Mach number of 2.0 the value would be 0.014 for inlet F and 0.025 for inlet C. With the assumption that the drag and thrust of the airplane at a Mach number of 2.0 would be equal, then, the drag coefficient for the airplane at a Mach number of 2.0 and 35,332-foot altitude would be about 0.052. (A thrust of 12,000 lb was selected from fig. 5(b) for two engines.) Then for inlet F the thrust loss resulting from the loss of pressure recovery is about 27 percent of the drag of the airplane while for inlet C the sum of the air-bypass drag, and the thrust loss resulting from the poor pressure recovery is about 49 percent of the airplane drag. If, by proper design of inlet F, the pressure recovery at a Mach number of 2.0 could be increased to 0.905, the value for best two-shock pressure recovery, the thrust-loss drag resulting from the pressure recovery would be reduced to about 14 percent of the drag of the airplane.

Inlet and Engine-Matching Considerations

For the purpose of discussion in this report, at supersonic speeds an inlet (or an air-induction system) is considered to be matched with the engine if the additive drag is zero when the weight of air delivered is that required by the engine. It is assumed that supercritical operation of the inlet is an unmatched condition. From the results of the preceding analysis of the operational characteristics of various inlets and the engine, it can be determined which of the inlets operates in a matched condition with the engine. It is apparent from figures 14 and 16 that only inlets D and F are matched with the engine throughout the speed range considered. Inlet B is matched with the engine only at a Mach number of 2.0, and the other inlets considered are not matched with the engine for Mach numbers between 1.0 and 2.0.

Matched operation, however, does not necessarily indicate the best performance. This is apparent from consideration of the drag summation for the inlets (fig. 15). As was noted above, inlets D and F are both matched with the engine throughout the speed range considered but the drag summation ΣK_D for inlet F is considerably lower than that for

inlet D at the higher Mach numbers. The difference between the drag summations of these two inlets is due entirely to the differences in their pressure recovery shown in figure 4. For Mach numbers above about 1.5 the performance of inlets A, B, and E is equal to or better than that for inlet D, even though the operation of inlets A, B, and E is not matched with the engine. From the preceding discussion it follows that the optimum combined performance of the inlet and engine results when the inlet is matched with the engine for the highest pressure recovery.

CONCLUDING REMARKS

An analysis has been made of several two-dimensional inlets intended for operation at Mach numbers up to 2.0 with aircraft powered by turbojet engines having constant volume air flow. A comparison of the inlets was made on the basis of factors accounting for the thrust loss due to loss of internal pressure recovery, additive drag, and air-bypass drag. The effects of viscosity (boundary layer) and the pressure drag of the external surfaces were not considered.

Of the factors considered in evaluating the relative performance of the inlets, it was shown that the thrust loss resulting from a loss of pressure recovery was the most significant. However, with certain inlets there were some off-design operating conditions where the additive drag was large. For the most part the drag of the air-bypass process was not large in relation to the additive and thrust-loss drag factors.

Except for certain types of variable-geometry inlets, it was apparent from the study that for the range of Mach numbers considered, an air-bypass system would be required with inlets operating with a turbojet engine having constant-volume air flow.

The performance of variable-geometry inlets was substantially better than that for similar type fixed-geometry inlets having equal pressure recovery. The variations with Mach number of entrance area and diffuser contraction required for ideal inlet-engine matching are indicated.

Ames Aeronautical Laboratory
National Advisory Committee for Aeronautics
Moffett Field, Calif., Aug. 3, 1953

APPENDIX A

ENGINE AIR-FLOW REQUIREMENTS

Using the definition of mass flow,

$$w_a = g \rho_o a_o A_{oR} M_o$$

(for matched operation $A_o = A_{oR}$) it follows that the ratio of A_{oR} at a free-stream Mach number to that at a Mach number of 1.0, for a constant altitude, is

$$\frac{(A_{oR})_{M_o}}{(A_{oR})_{M_o=1.0}} = \frac{(M_o)_{M_o=1.0}}{(M_o)_{M_o}} \frac{(w_a)_{M_o}}{(w_a)_{M_o=1.0}} \quad (A1)$$

Also, from the continuity of flow

$$w_a = g \rho_3 a_3 A_3 M_3$$

Assuming that the air flows through the engine at a constant volume rate at rated rpm and that there is no loss of total pressure or total temperature in the air-induction system, then

$$\frac{(w_a)_{M_o}}{(w_a)_{M=1.0}} = \frac{(\rho_3)_{M_o}}{(\rho_3)_{M_o=1.0}}$$

Thus, for a ratio of specific heats for air of 1.4,

$$\frac{(w_a)_{M_o}}{(w_a)_{M_o=1.0}} = \frac{(1+0.2M_o^2)_{M_o}^{5/2}}{(1+0.2M_o^2)_{M_o=1.0}^{5/2}} \frac{(1+0.2M_3^2)_{M_o=1.0}^{5/2}}{(1+0.2M_3^2)_{M_o}^{5/2}} \quad (A2)$$

Combining equations (A1) and (A2) gives

$$\frac{(A_{oR})_{M_o}}{(A_{oR})_{M_o=1.0}} = \frac{(M_o)_{M_o=1.0}}{(M_o)_{M_o}} \frac{(1+0.2M_o^2)_{M_o}^{5/2}}{(1+0.2M_o^2)_{M_o=1.0}^{5/2}} \frac{(1+0.2M_3^2)_{M_o=1.0}^{5/2}}{(1+0.2M_3^2)_{M_o}^{5/2}} \quad (A3)$$

To use this equation to calculate the free-stream area as a function of free-stream Mach number, it is necessary that the Mach number at

station 3 be known. Use of equation (1) shows that

$$\frac{(A_{OR})_{M_0}}{(A_{OR})_{M_0=1.0}} = \frac{(M_0)_{M_0=1.0}}{(M_0)_{M_0}} \frac{(1+0.2M_0^2)_{M_0}^3}{(1+0.2M_0^2)_{M_0=1.0}^3} \frac{(w_{ac})_{M_0}}{(w_{ac})_{M_0=1.0}} \quad (A4)$$

(It is evident by inspection, with proper regard to notation and Mach number, that eqs. (A4) and (B8) of ref. 4 are the same.) With this equation the corrected air flow must be known to calculate A_{OR} . The calculation of A_{OR} by use of either equation (A3) or (A4) is lengthy and tedious. The calculations can be simplified if it is assumed that the weight of flow is proportional to the stagnation density at the compressor. Thus,

$$\frac{(w_a)_{M_0}}{(w_a)_{M_0=1.0}} = \frac{(1+0.2M_0^2)_{M_0}^{5/2}}{(1+0.2M_0^2)_{M_0=1.0}^{5/2}}$$

Then,

$$\frac{(A_{OR})_{M_0}}{(A_{OR})_{M_0=1.0}} = \frac{(M_0)_{M_0=1.0}}{(M_0)_{M_0}} \frac{(1+0.2M_0^2)_{M_0}^{5/2}}{(1+0.2M_0^2)_{M_0=1.0}^{5/2}} \quad (A5)$$

The similarity between equations (A3) and (A5) is obvious. As long as the variation of Mach number at the compressor is small, the quantity

$$\frac{(1+0.2M_3^2)_{M_0=1.0}^{5/2}}{(1+0.2M_3^2)_{M_0}^{5/2}} \approx 1.0$$

The variation of A_{OR} is, consequently, defined by equation (A5). For the engine of this study, equation (A5) defines the air-flow characteristics presented in figure 7 for a total pressure recovery of 1.0. Calculation of A_{OR} by equation (A3) does not differ greatly. For example, at a free-stream Mach number of 1.6 and an altitude of 35,332 feet, the values of A_{OR} as calculated by equations (A5) and (A3) are 1.66 and 1.69, respectively; at a Mach number of 2.0 the values are 2.06 and 2.13, respectively.

APPENDIX B

FURTHER CONSIDERATIONS OF INLET F

Matched operation of the inlet with the engine for a condition of high pressure recovery is possible with the design features of inlet F, that is, convergent-divergent diffuser, variable contraction ratio, and variable entrance area. To show that higher pressure recoveries than were assumed are probable with inlet F, and to indicate how such an inlet may operate, some calculations of inlet geometry and shock-wave configurations were made. In figure 17 sketches show the geometry of the inlet and the associated shock-wave pattern for free-stream Mach numbers of 2.0, 1.8, 1.6, and 1.4. In each case a normal shock wave was assumed to occur immediately behind the minimum-area section. Pertinent data related to the geometry of the inlet and to the characteristics of the air flow are tabulated in figure 17 for each of the free-stream Mach numbers.

The basic geometry of the inlet, that is, the entrance area, the length between the entrance and the section of minimum area, and the thickness of the lip at the section of minimum area is determined from the assumptions made for the highest speed ($M_0 = 2.0$). Since A_{OR} , A_0 , and A_e must be equal, the entrance area can be determined by using equation (1). (The assumed total-pressure ratios H_3/H_0 are shown in fig. 17.) The calculated values of A_{OR} apply for altitudes within the stratosphere. The assumed total-pressure ratios H_3/H_0 are considerably higher than the values considered for inlet F in the preceding analysis (fig. 4) for corresponding Mach numbers and represent values to be achieved with proper over-all diffuser design. (That such high pressure recoveries might actually be realized is indicated in reference 10; high pressure recoveries were obtained in experiments with properly designed convergent-divergent perforated diffusers.) The length required between the entrance and the section of minimum area depends on the shock-wave pattern at a Mach number of 2.0. For the purposes of this analysis it was assumed that the flow deflection angles δ and δ_l (fig. 17) were equal and of such values that the oblique shock waves from the lip and from the ramp in the floor of the inlet would each reflect once ahead of the minimum-area section in such a way that the reflected waves then would each intersect the opposite surface of the inlet at the minimum-area section. (See the sketch in fig. 17 for $M_0 = 2.0$.) To satisfy this shock-wave pattern, the internal geometry of the inlet ahead of the minimum-area section would have to be symmetrical in the two-dimensional plane. Then the length of the inlet and the contraction ratio A_0/A_m would each have a specific value. If the external surface of the lip is assumed parallel to the free-stream direction, then the thickness of the lip at the minimum section can be calculated.

When operating at a free-stream Mach number of 2.0, the flow would be symmetrical within the inlet (because of the geometric symmetry) so that the flow in regions a, c, e, and g (fig. 17) would be the same as the flow in regions b, d, f, and h. The total-pressure ratio H_m/H_0 available at the minimum-area section was calculated from considerations of the shock-wave patterns, and the values are shown also in figure 17.

At free-stream Mach numbers less than 2.0 the lip must be rotated to decrease the entrance area from its value at $M_0 = 2.0$ to a value corresponding to A_{OR} for a particular free-stream Mach number. Then the flow deflection angle, δ_l , caused by the lip is decreased from its value at $M_0 = 2.0$. (See fig. 17 for $M_0 = 1.8$.) If flow symmetry is to be maintained (as was assumed in this analysis for $M_0 = 2.0$ and 1.8), the ramp on the floor of the inlet must be lowered so that the flow deflection angle δ is the same as δ_l . The sketch in figure 17 shows this type of operation for a free-stream Mach number of 1.8, and also the computed values for the total-pressure ratio H_m/H_0 and the contraction ratio A_0/A_m .

At some free-stream Mach numbers the pressure recovery available at the minimum-area section may be reduced if the geometry is varied to obtain flow symmetry, because the flow deflection angles (contraction ratio) may be too small to reduce the Mach number of the entering flow to near 1.0 at the minimum-area section. (In order to obtain a high pressure recovery the Mach number of the flow entering the inlet must be reduced so that the normal shock wave at the minimum-area section occurs at a Mach number of about 1.0.) Thus, at a free-stream Mach number of 1.6 A_{OR} is such that high pressure recovery cannot be obtained by varying the geometry of the inlet to obtain flow symmetry. To obtain better pressure recovery the ramp in the floor of the inlet can be changed so as to increase the flow deflection angle δ . Then the contraction ratio is increased and the flow becomes unsymmetrical, as indicated in figure 17 for $M_0 = 1.6$. A limiting condition for the flow deflection angle caused by the lip or the ramp in the floor of the inlet is that the flow deflection angle (δ , δ_l) must not be so large as to cause any of the shock waves ahead of the minimum-area section to become detached. Because of the unsymmetrical flow, a small region of vorticity may occur with the mixing of dissimilar flows behind the shock waves from the lip and floor of the inlet (regions c and d, and g and h in the sketch for $M_0 = 1.6$, fig. 17). Reference 11 discusses some aspects of this type of flow. The pressure recovery for this type of flow may actually be less than the value shown in figure 17 which was calculated from the shock-wave considerations alone. However, because the flow direction and static pressure within two mixing regions (c and d, or g and h) are the same and, because the velocities in the two regions will not differ greatly, it would seem that the pressure loss should not be large.

At a Mach number of 1.4 A_{OR} has decreased so much that the flow deflection caused by the lip is no longer compressive (δ_l is negative in sense) and expansion would occur around the leading edge of the inner surface of the lip. Because δ_l is so small at a Mach number of 1.4, the expansion was neglected in this analysis. At lower Mach numbers δ_l would be larger and further consideration would have to be given to the effect of the expansion. To obtain high pressure recovery the floor of the inlet must be changed to give the desired contraction ratio and shock-wave pattern as indicated in the sketch for $M_0 = 1.4$ (fig. 17).

For the purposes of this analysis of inlet F it was assumed that at a given free-stream Mach number, the difference between the assumed total-pressure ratio H_3/H_0 and the total-pressure ratio H_m/H_0 calculated from the shock-wave pattern would correspond to a subsonic diffuser loss. Consideration of the contraction ratios shown in figure 17 and the variation of contraction ratio with Mach number shown in figure 11 indicates that the values shown in figure 17 approach, in general, the isentropic values for the particular Mach number. Operation of the inlet to keep the contraction ratios near the isentropic value, or the value required for a particular multishock configuration, should result in high pressure recovery.

Besides the potential for matched operation with the engine for a condition with high pressure recovery, inlet F possesses other desirable qualities. Features to improve the performance of the inlet can be incorporated in its geometry. The design of the diverging portion of the diffuser could be such as to include a long section of nearly constant area which should act to stabilize the flow within the inlet. (Ref. 12 indicates the need in this respect for a long diffuser section with nearly constant area following the minimum-area section.) With supersonic flow stabilized within the inlet, the contraction ratio can be varied to approach the value required for isentropic compression. During take-off a large entrance area is needed and the inlet can be opened to take in more air, perhaps eliminating the necessity for additional air-access openings. With the inlet wide open the difficulties ordinarily associated with separation of the flow from the internal surfaces of sharp lips might be minimized. The geometry of inlet F could be adapted to an inlet of rectangular design; it could be used as a nose inlet, fuselage side inlet, in pod arrangement, etc.

The considerations presented herein point out the possible advantages of inlets such as F for flight through the Mach number range up to 2.0; however, a true evaluation must await experiments with inlets of this type. One large disadvantage of inlet F is, of course, the mechanical complexities involved in varying the geometry so that the air-induction system and engine can be operated properly. It remains for future investigation to determine the effects on over-all inlet performance of wave drag, of the third dimension, of viscous flow, etc., for the probable configurations of inlet F.

REFERENCES

1. Blackaby, James R.: An Analytical Study of the Comparative Performance of Four Air-Induction Systems for Turbojet-Powered Airplanes Designed to Operate at Mach Numbers up to 1.5. NACA RM A52C14, 1952.
2. Sturdevant, C. R., and Woodworth, L. R.: A Generalized Turbojet Weight, Size, and Performance Study. The Rand Corporation, R-166, Dec. 1949.
3. The Staff of the Ames 1- by 3-Foot Supersonic Wind-Tunnel Section: Notes and Tables for Use in the Analysis of Supersonic Flow. NACA TN 1428, 1947.
4. Brajnikoff, George B.: Method and Graphs for the Evaluation of Air-Induction Systems. NACA TN 2697, 1952.
5. Schueller, Carl F., and Esenwein, Fred T.: Analytical and Experimental Investigation of Inlet-Engine Matching for Turbojet-Powered Aircraft at Mach Numbers up to 2.0. NACA RM E51K20, 1952.
6. Klein, Harold: The Calculation of the Scoop Drag for a General Configuration in a Supersonic Stream. Douglas Rep. SM-13744, Apr. 1950.
7. Sibulkin, Merwin: Theoretical and Experimental Investigation of Additive Drag. NACA RM E51B13, 1951.
8. Moeckel, W. E.: Approximate Method for Predicting Form and Location of Detached Shock Waves Ahead of Plane or Axially Symmetric Bodies. NACA TN 1921, 1949.
9. Allen, J. L., and Beke, Andrew: Force and Pressure Recovery Characteristics at Supersonic Speeds of a Conical Spike Inlet with a Bypass Discharging from the Top or Bottom of the Diffuser in an Axial Direction. NACA RM E53A29, 1953.
10. Hunczak, Henry R., and Kremzier, Emil J.: Characteristics of Perforated Diffusers at Free-Stream Mach Number 1.90. NACA RM E50B02, 1950.
11. Ferri, Antonio: Elements of Aerodynamics of Supersonic Flows. The MacMillan Company, New York, 1949.
12. Lustwerk, Ferdinand: The Influence of Boundary Layer on the "Normal" Shock Configurations. MIT Meteor Rep. 61. (Guided Missiles Program, Bureau of Ordnance, Navy Dept.) Sept. 1950.

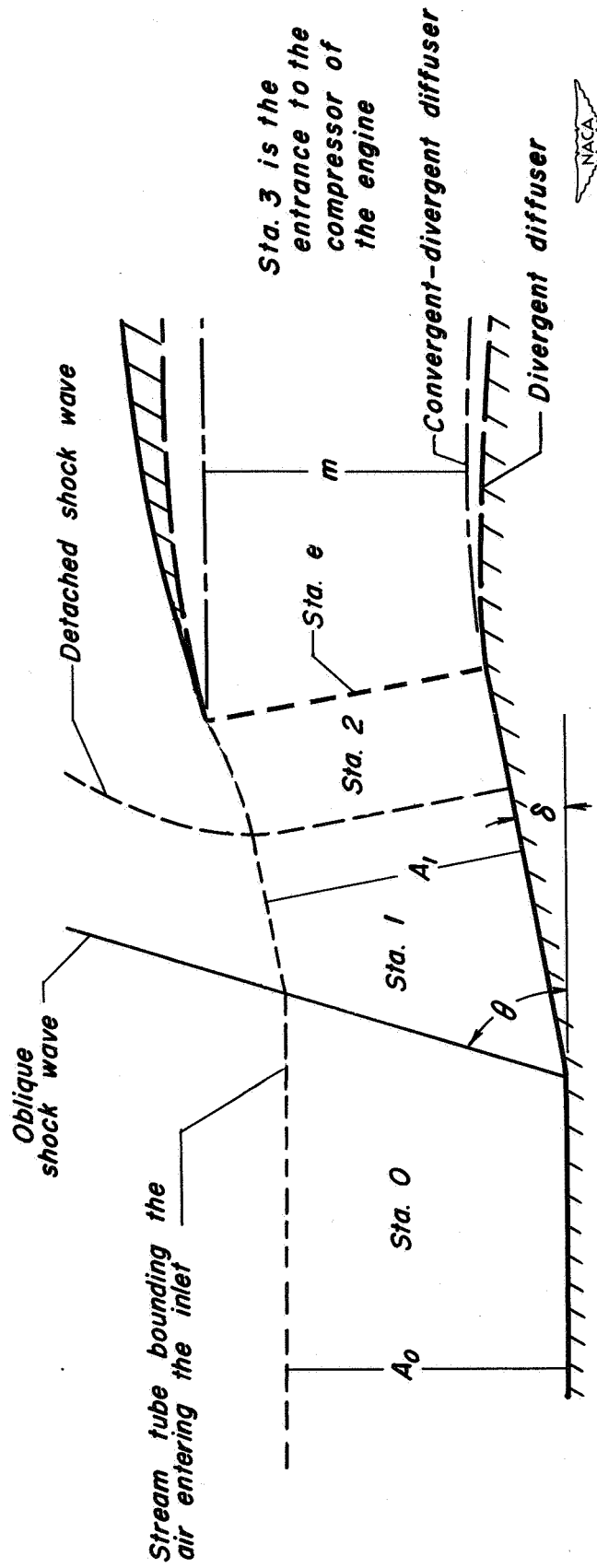


Figure 1.- Nomenclature.

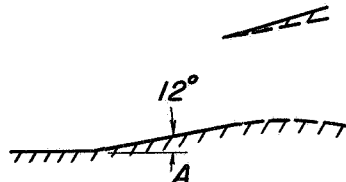
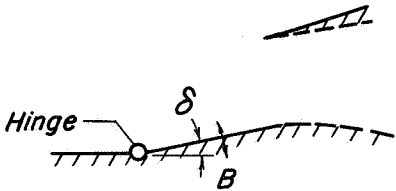
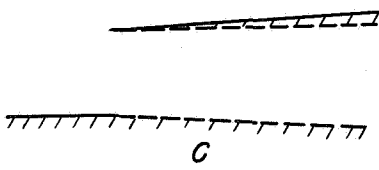
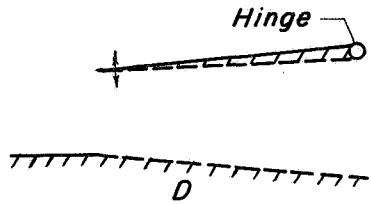
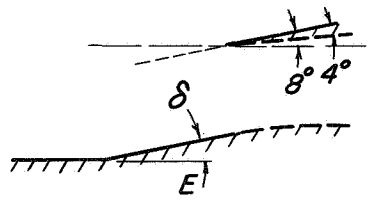
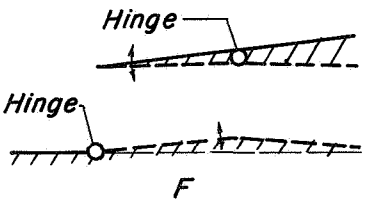
Inlets	Description
	<p>Ramp angle - Constant, 12°</p> <p>Entrance area - Constant, 1.480 sq ft</p> <p>Diffuser - Divergent</p>
	<p>Ramp angle - Variable</p> <p>Entrance area - Variable</p> <p>Diffuser - Divergent</p>
	<p>Ramp angle - Constant, 0°</p> <p>Entrance area - Constant, 1.480 sq ft</p> <p>Diffuser - Divergent</p>
	<p>Ramp angle - Constant, 0°</p> <p>Entrance area - Variable</p> <p>Diffuser - Divergent</p>
	<p>Ramp angle - Constant, $8^\circ 4'$</p> <p>Entrance area - Constant, 1.590 sq ft</p> <p>Diffuser - Convergent-divergent</p>
	<p>Ramp angle - Constant, 0°</p> <p>Entrance area - Variable</p> <p>Diffuser - Variable</p>



Figure 2.- Schematic diagrams and descriptions of the inlets.

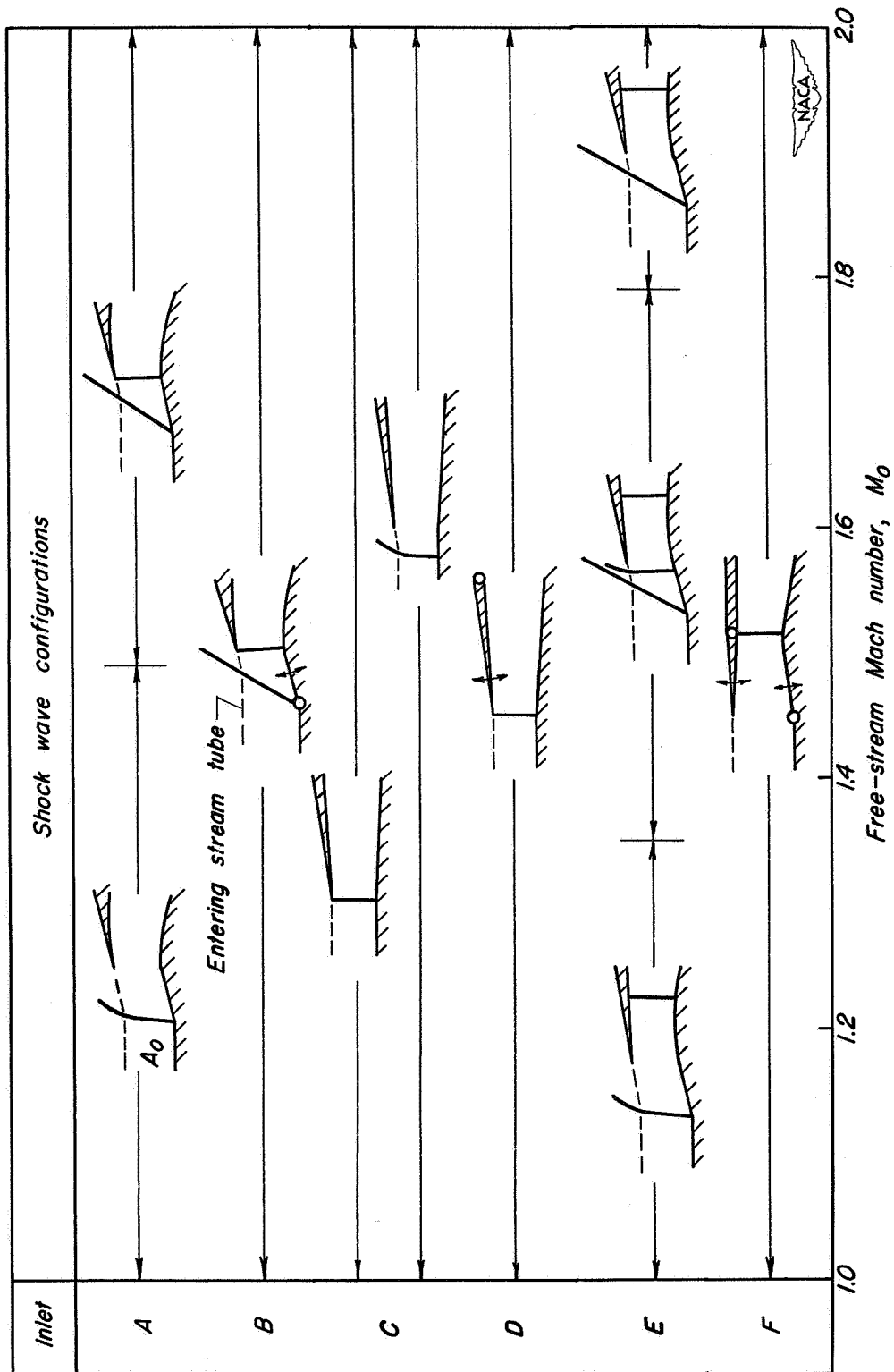


Figure 3.- Diagrammatic representations of the shock-wave configurations for each of the inlets.

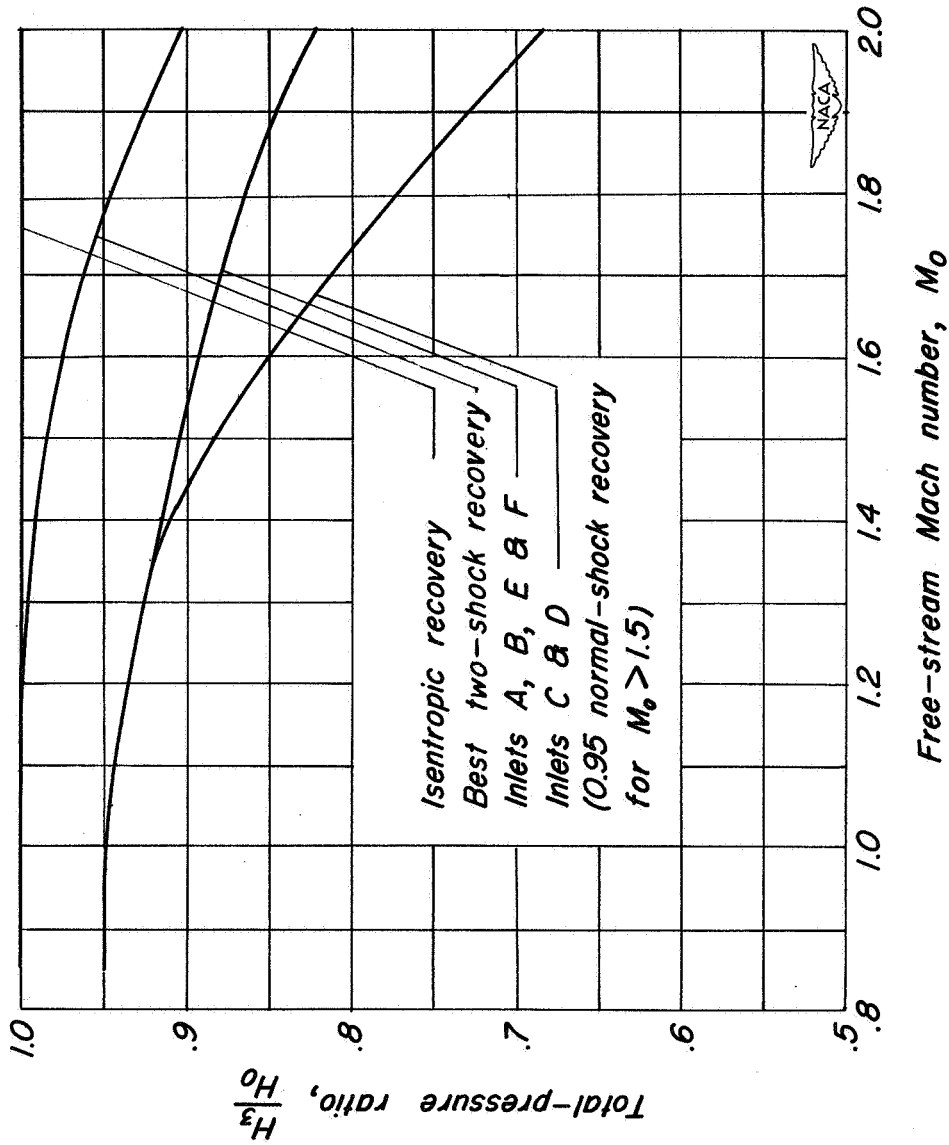
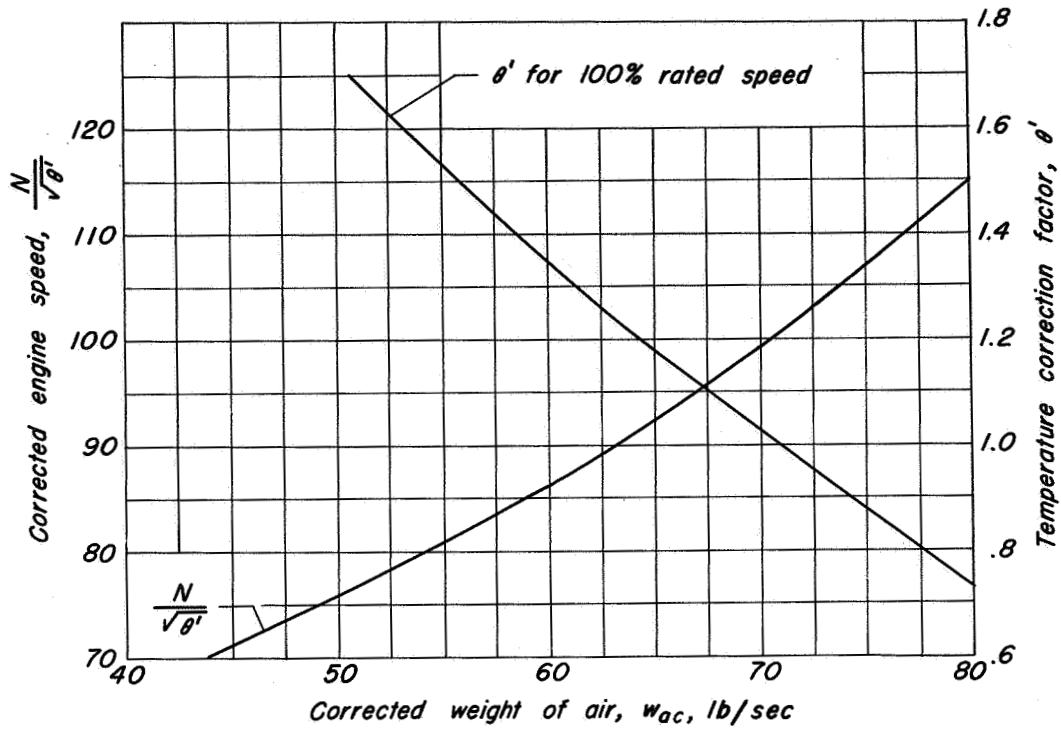
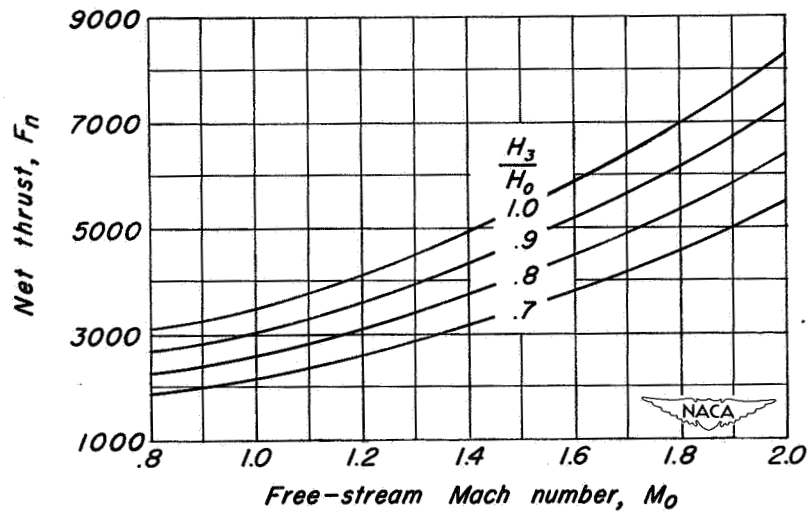


Figure 4.- The variation of total-pressure ratio with free-stream Mach number for each of the inlets, and for different flow conditions.



(a) Corrected air flow.



(b) Net thrust, rated rpm with afterburning, altitude 35,332 feet.

Figure 5.- Corrected air flow and net thrust for the assumed turbojet engine.

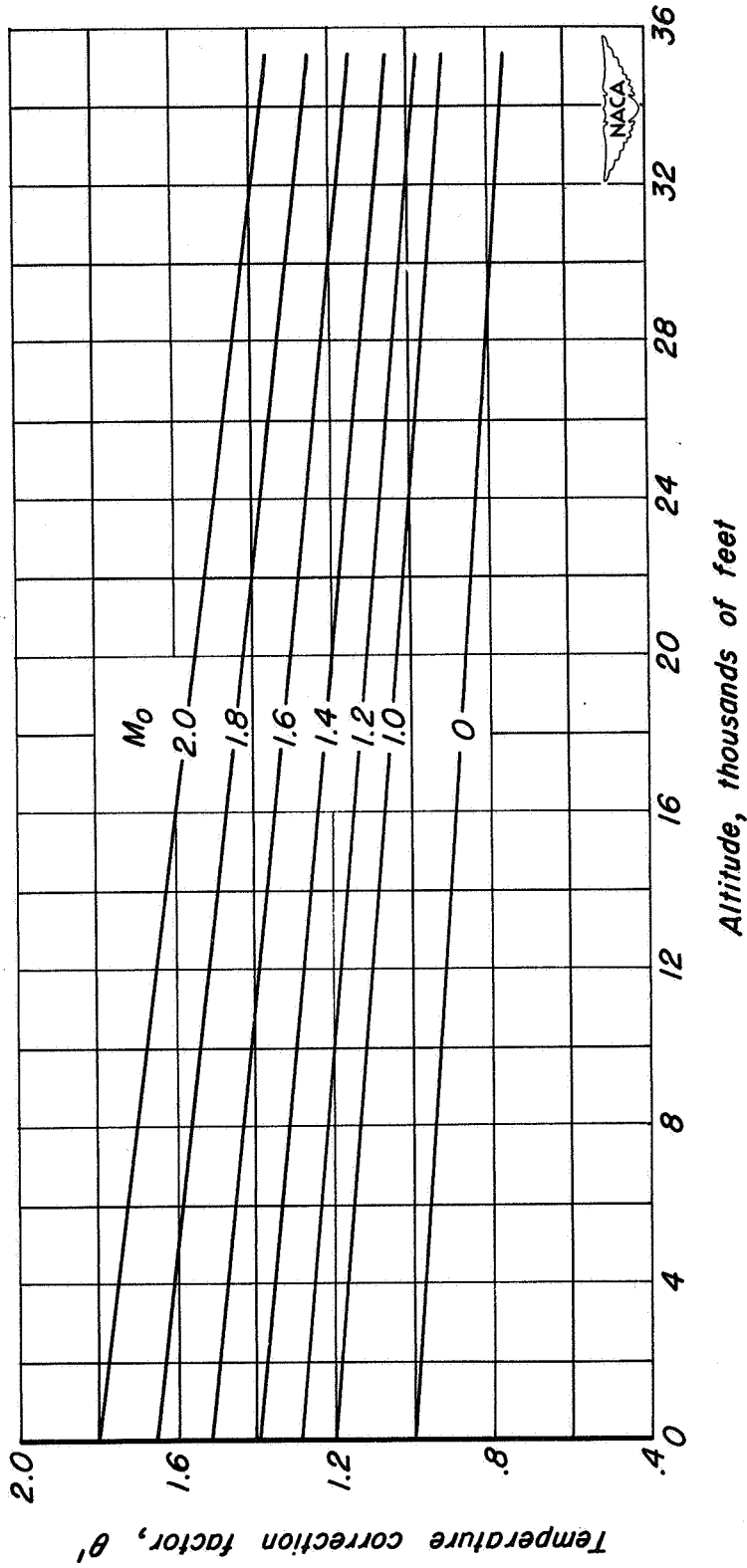


Figure 6.- The variation of the temperature correction factor with altitude and free-stream Mach number.

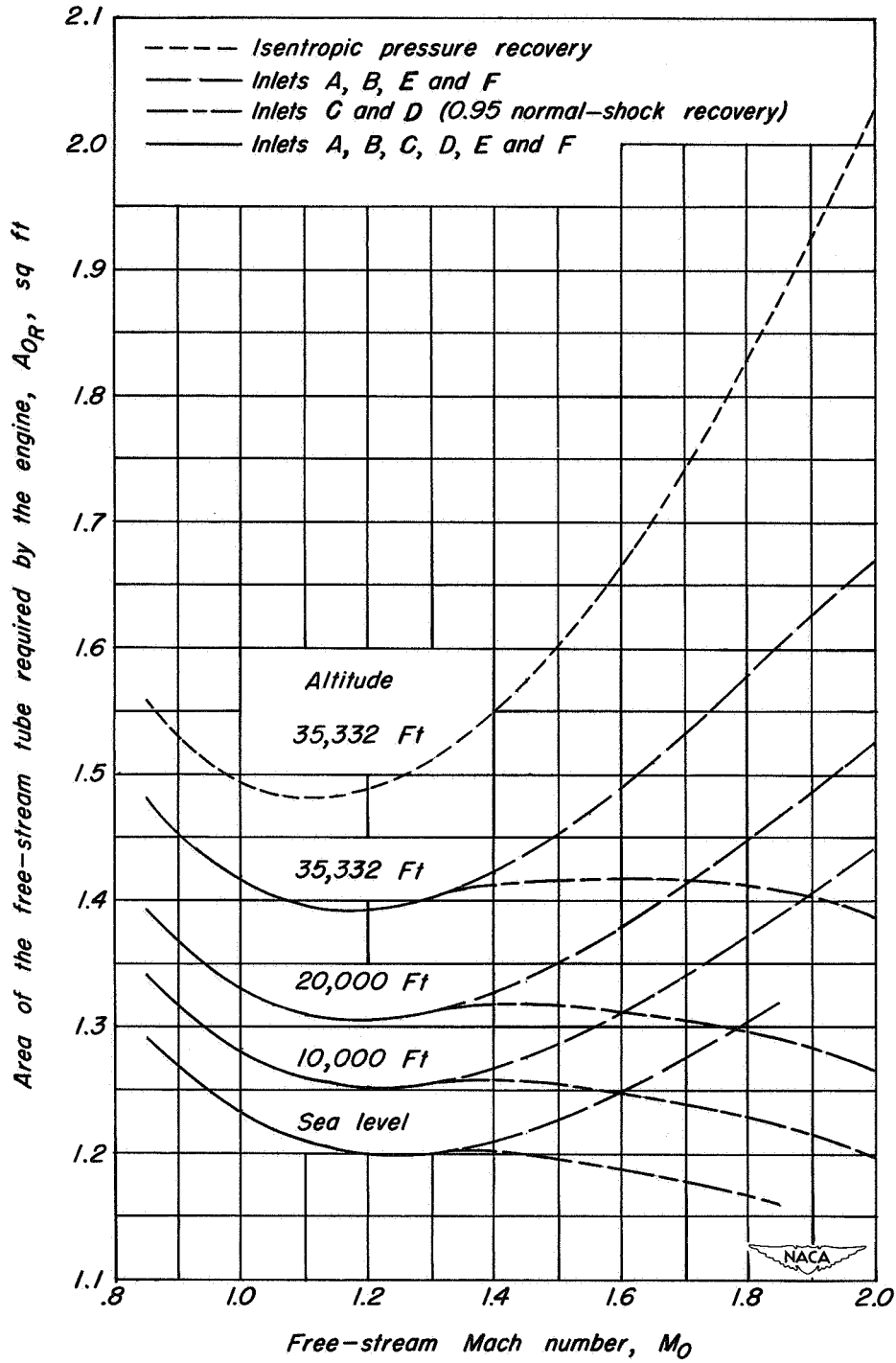
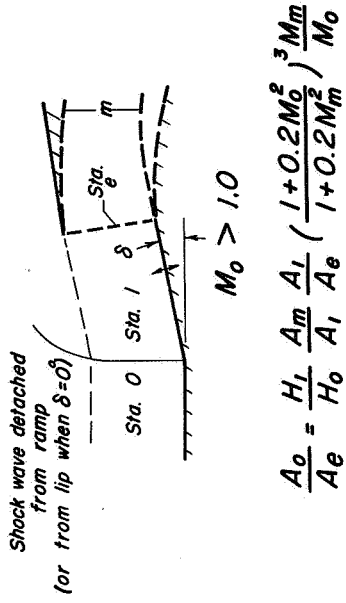


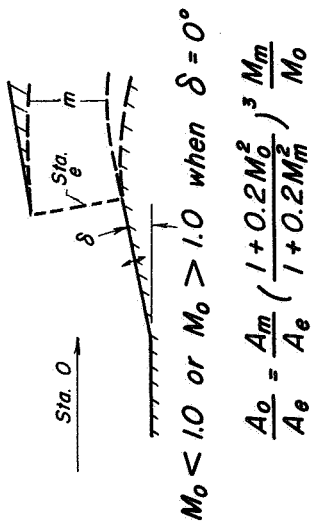
Figure 7.- The area of the free-stream-tube required by the engine for various free-stream Mach numbers, altitudes, and pressure recoveries.



$$\frac{A_0}{A_e} = \frac{H_1}{H_0} \frac{A_m}{A_1} \frac{A_1}{A_e} \left(\frac{1+0.2M_0^2}{1+0.2M_m^2} \right)^3 \frac{M_m}{M_0}$$

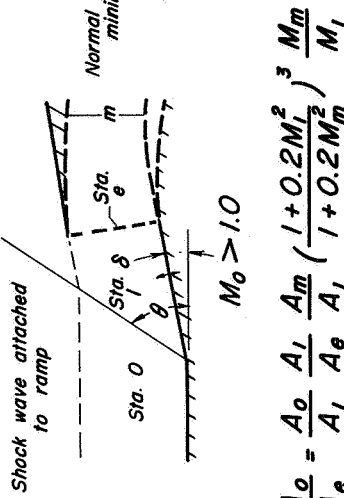
Eq. (2b).

Note: When the diffuser is divergent, m and e coincide and the equations can be simplified.



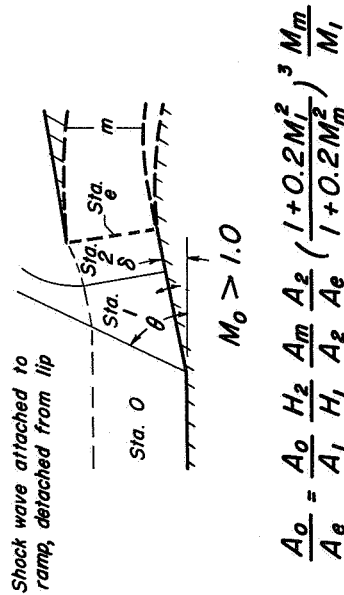
$$\frac{A_0}{A_e} = \frac{A_m}{A_e} \left(\frac{1+0.2M_0^2}{1+0.2M_m^2} \right)^3 \frac{M_m}{M_0}$$

Eq. (2a).



$$\frac{A_0}{A_e} = \frac{A_0}{A_1} \frac{A_1}{A_e} \frac{A_m}{A_1} \left(\frac{1+0.2M_1^2}{1+0.2M_m^2} \right)^3 \frac{M_m}{M_1}$$

Eq. (2d).



$$\frac{A_0}{A_e} = \frac{A_0}{A_1} \frac{H_2}{H_1} \frac{A_m}{A_2} \frac{A_2}{A_e} \left(\frac{1+0.2M_1^2}{1+0.2M_m^2} \right)^3 \frac{M_m}{M_1}$$

Eq. (2c).

Figure 8.- Forms of the equation for mass-flow ratio.



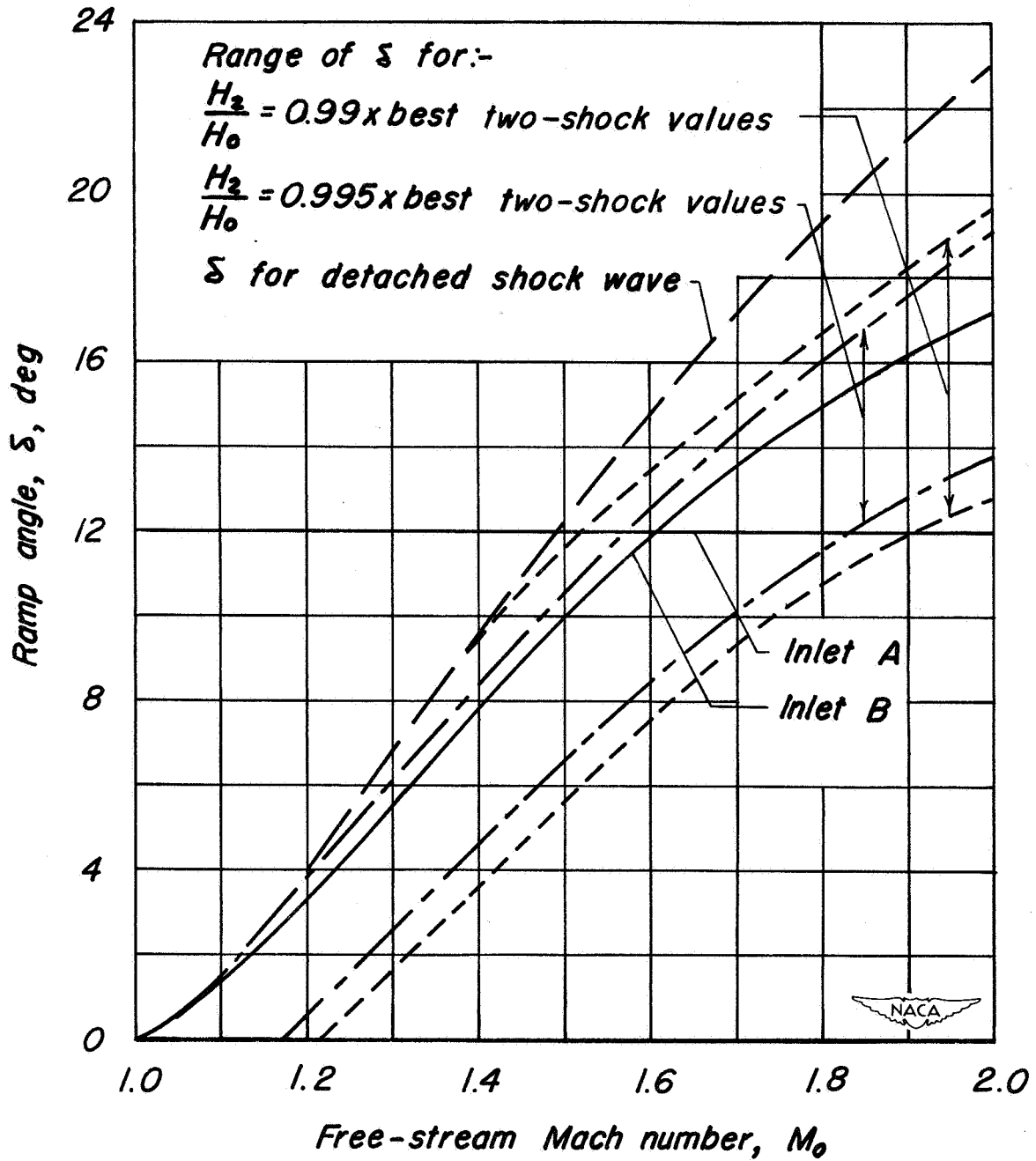
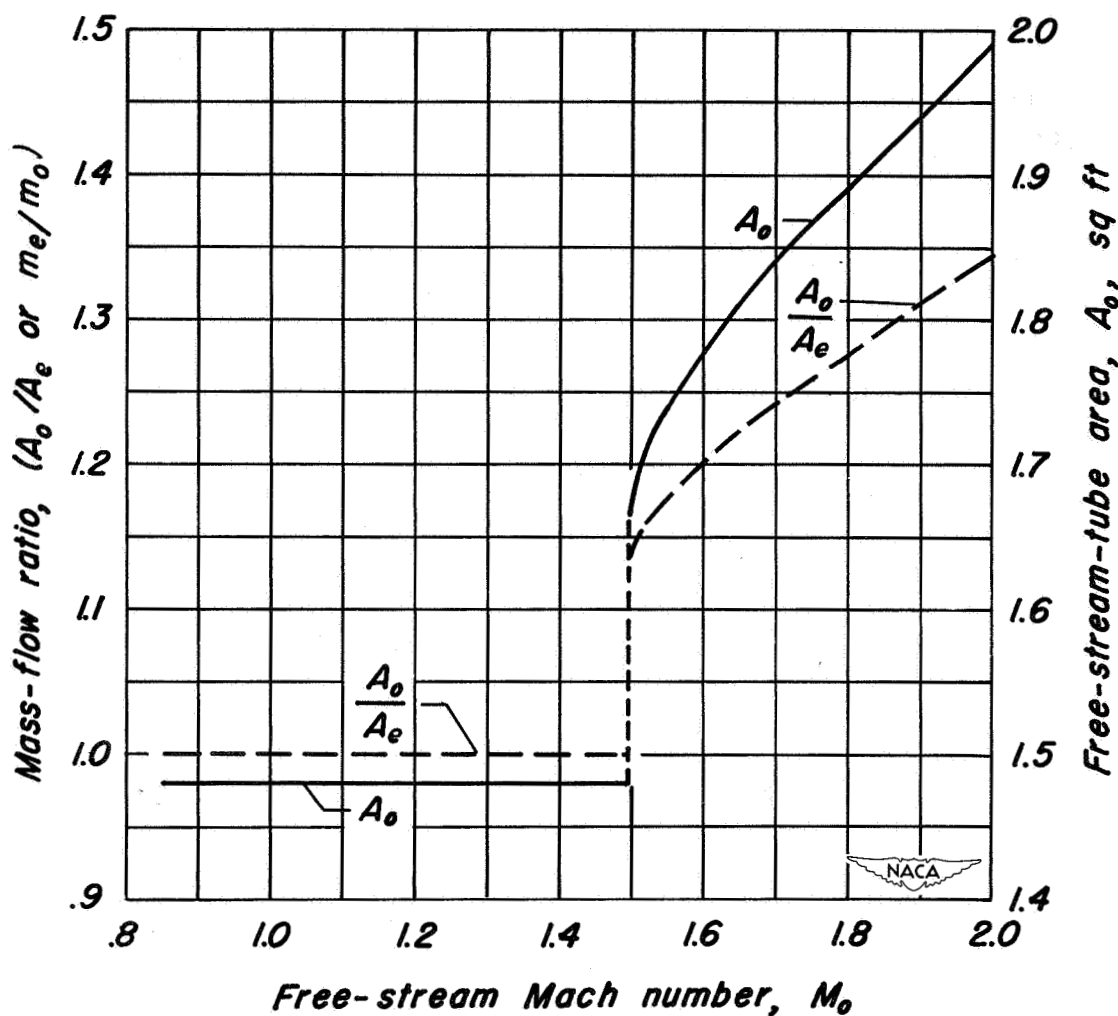
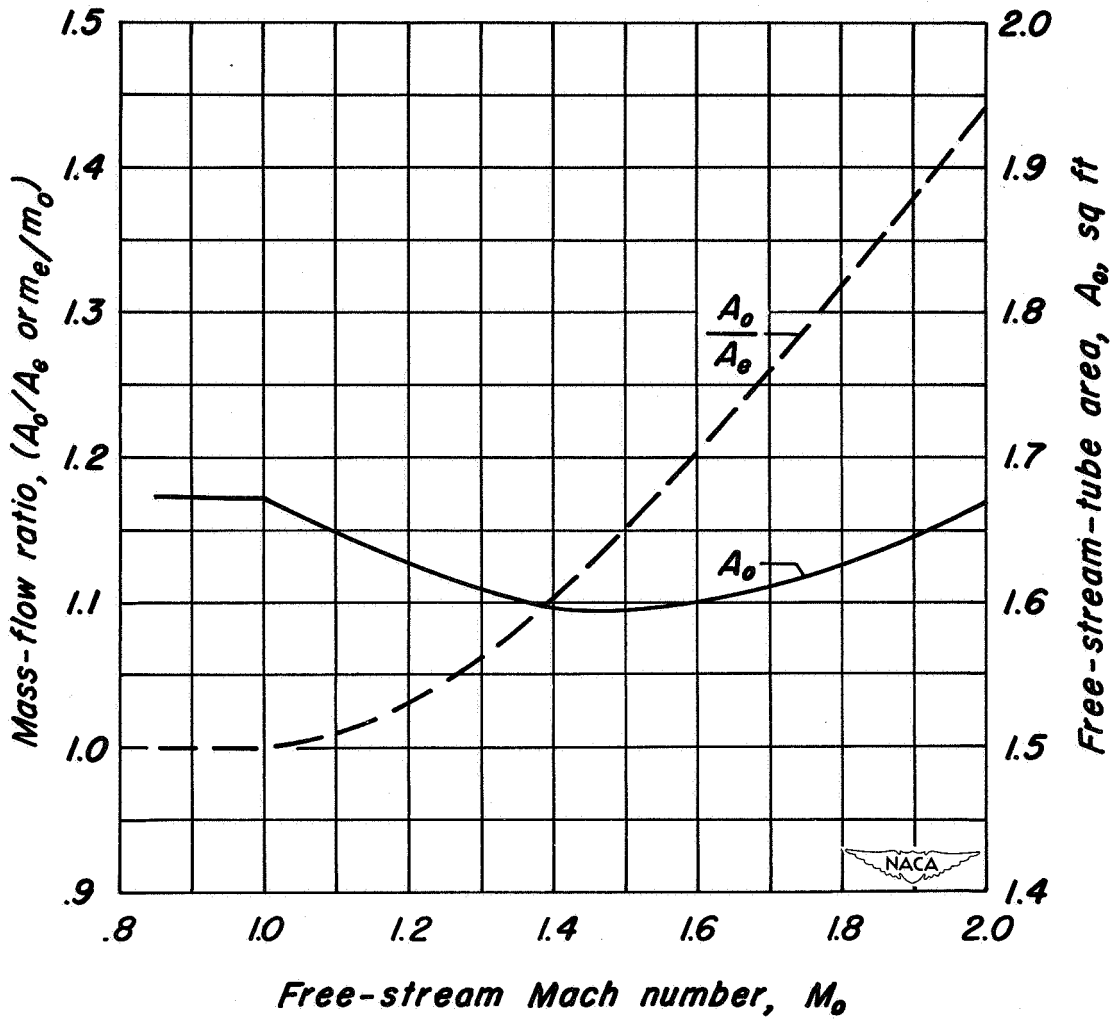


Figure 9.- The range of ramp angles for pressure recovery near that for best two-shock recovery for free-stream Mach numbers between 1.0 and 2.0.



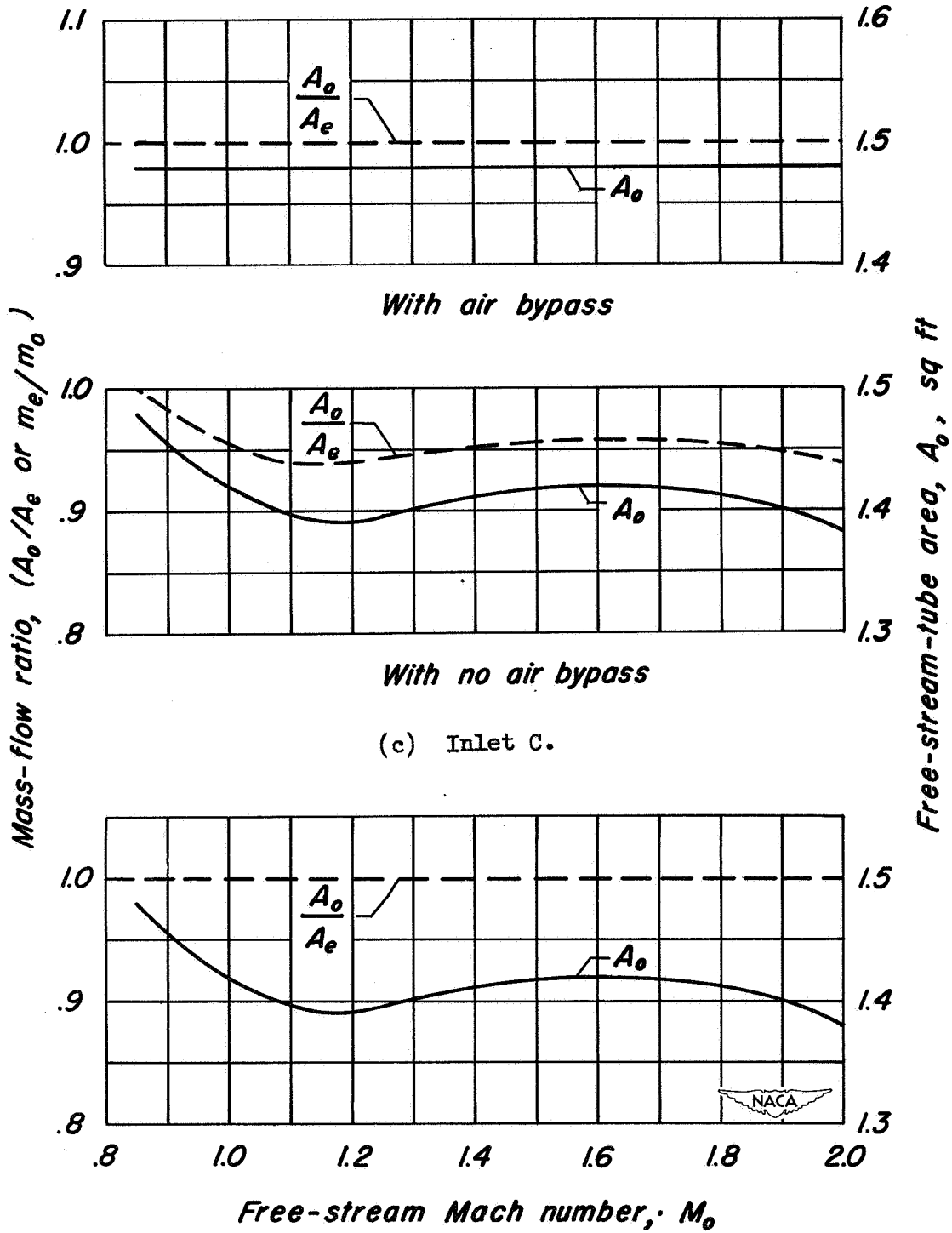
(a) Inlet A.

Figure 10.- The variation with free-stream Mach number of mass-flow ratio, and free-stream-tube area A_0 for each of the inlets.



(b) Inlet B.

Figure 10.- Continued.



(c) Inlet C.

(d) Inlet D.

Figure 10.- Continued.

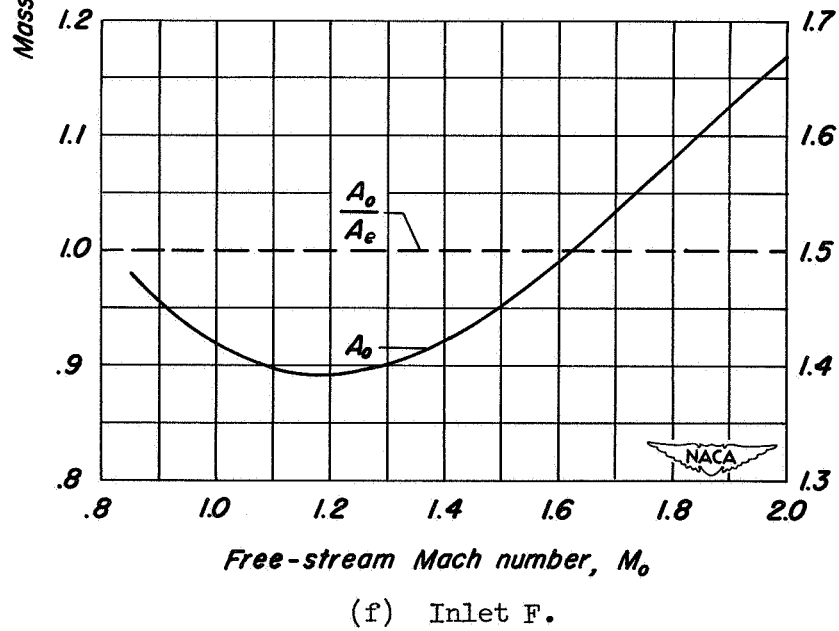
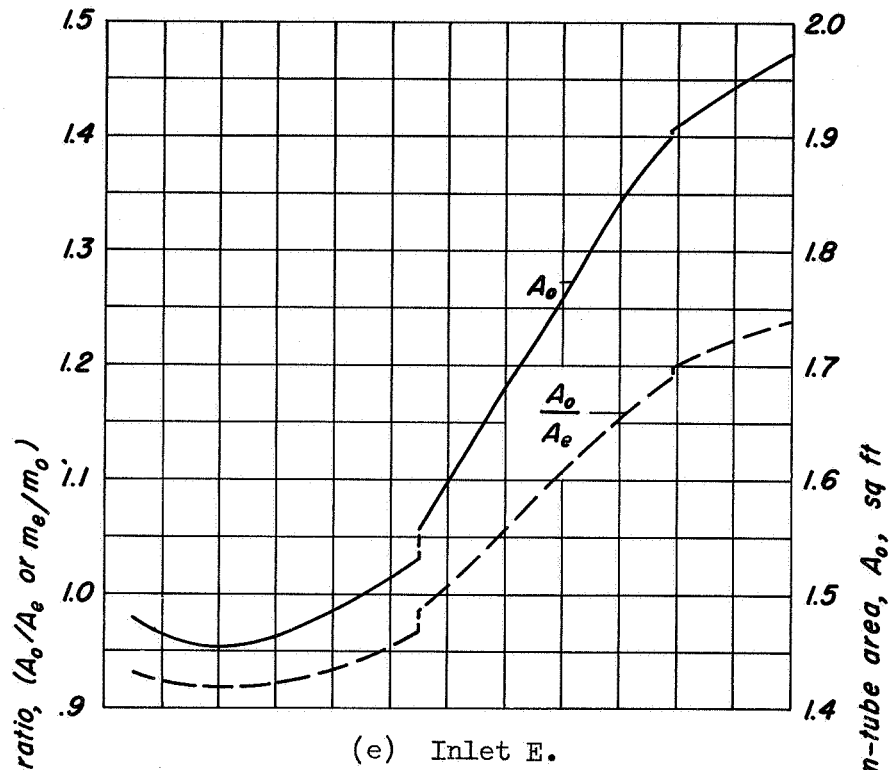


Figure 10.- Concluded.

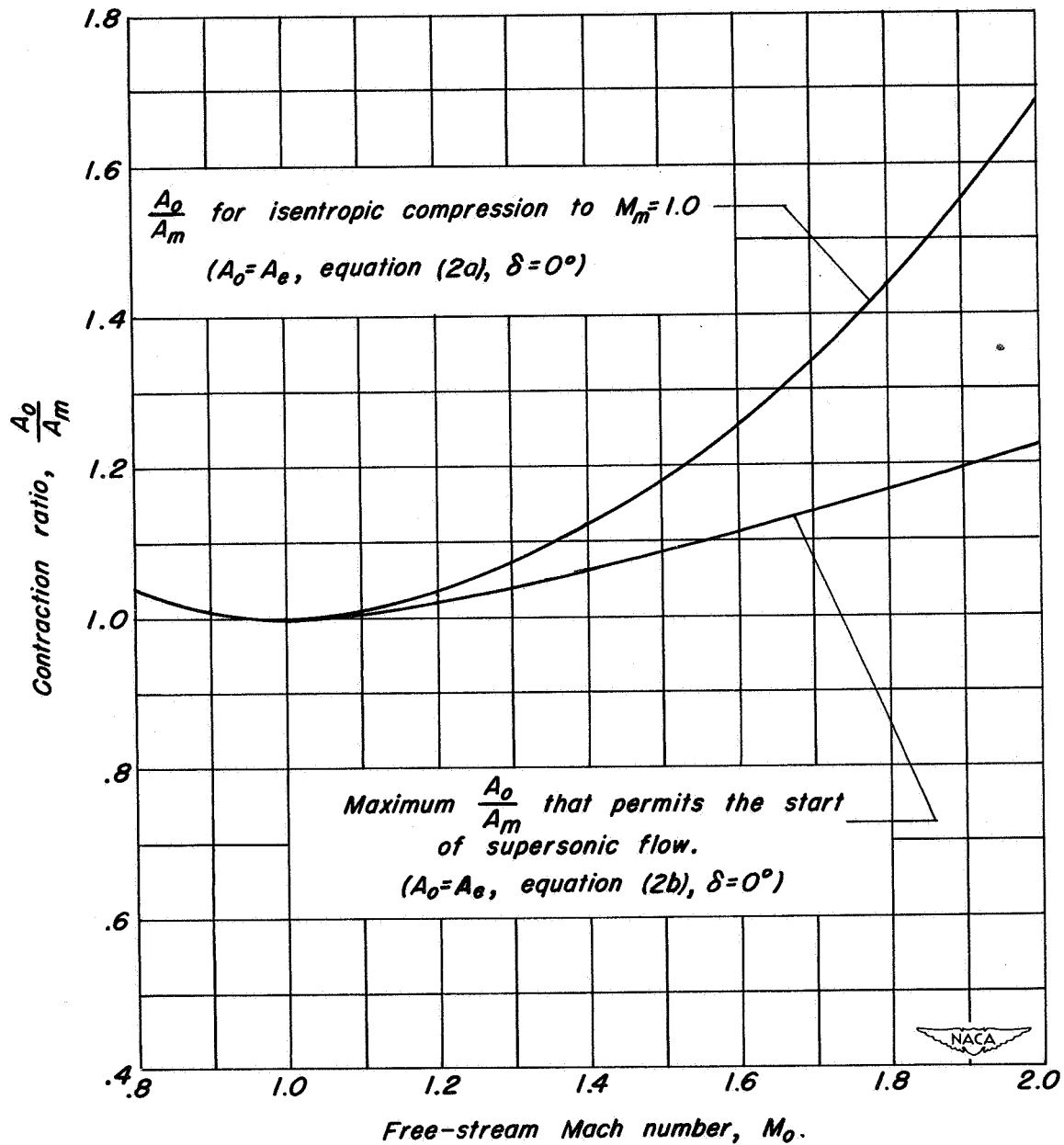


Figure 11.- The variation of the contraction ratio A_0/A_m with free-stream Mach number for $M_m = 1.0$.

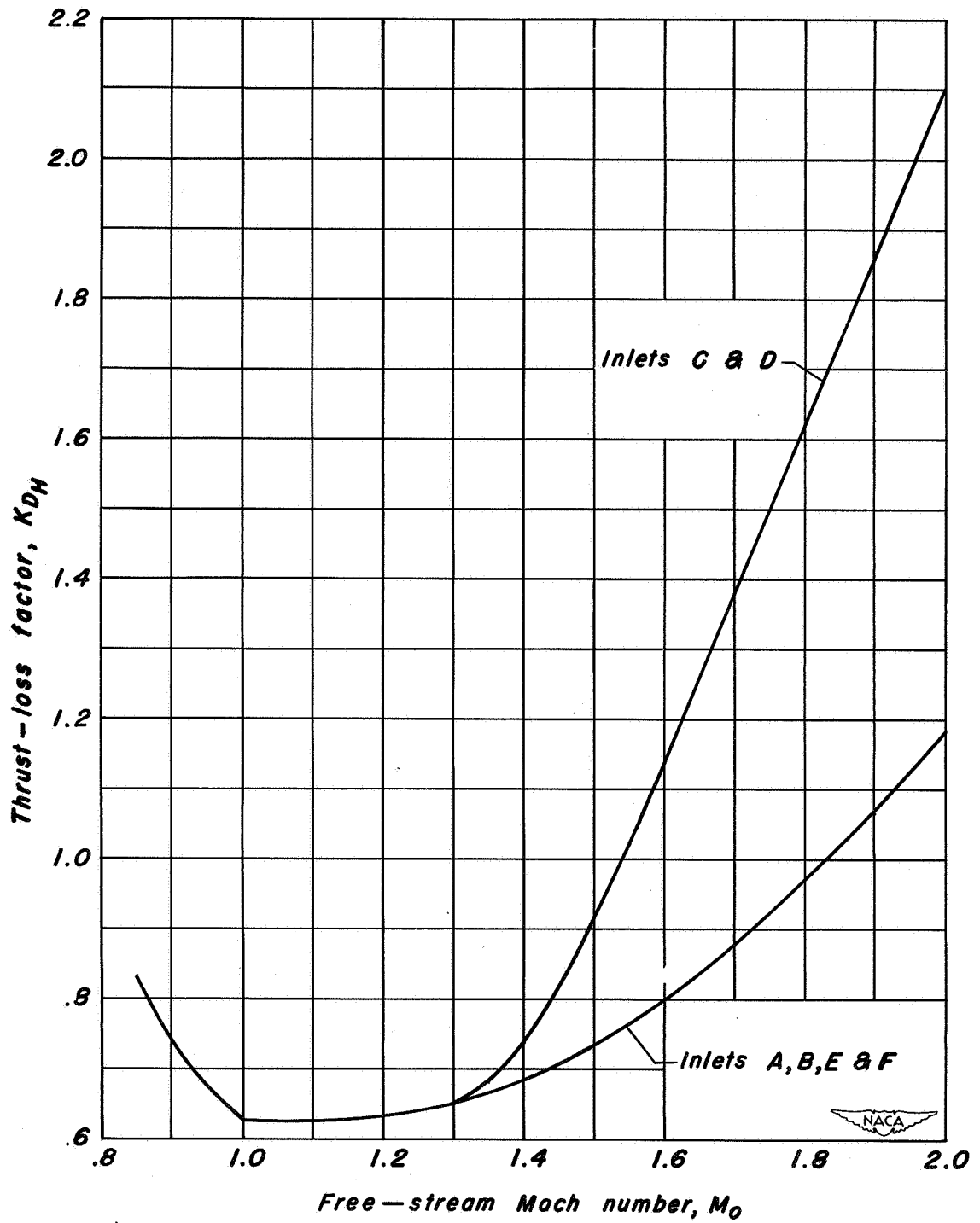
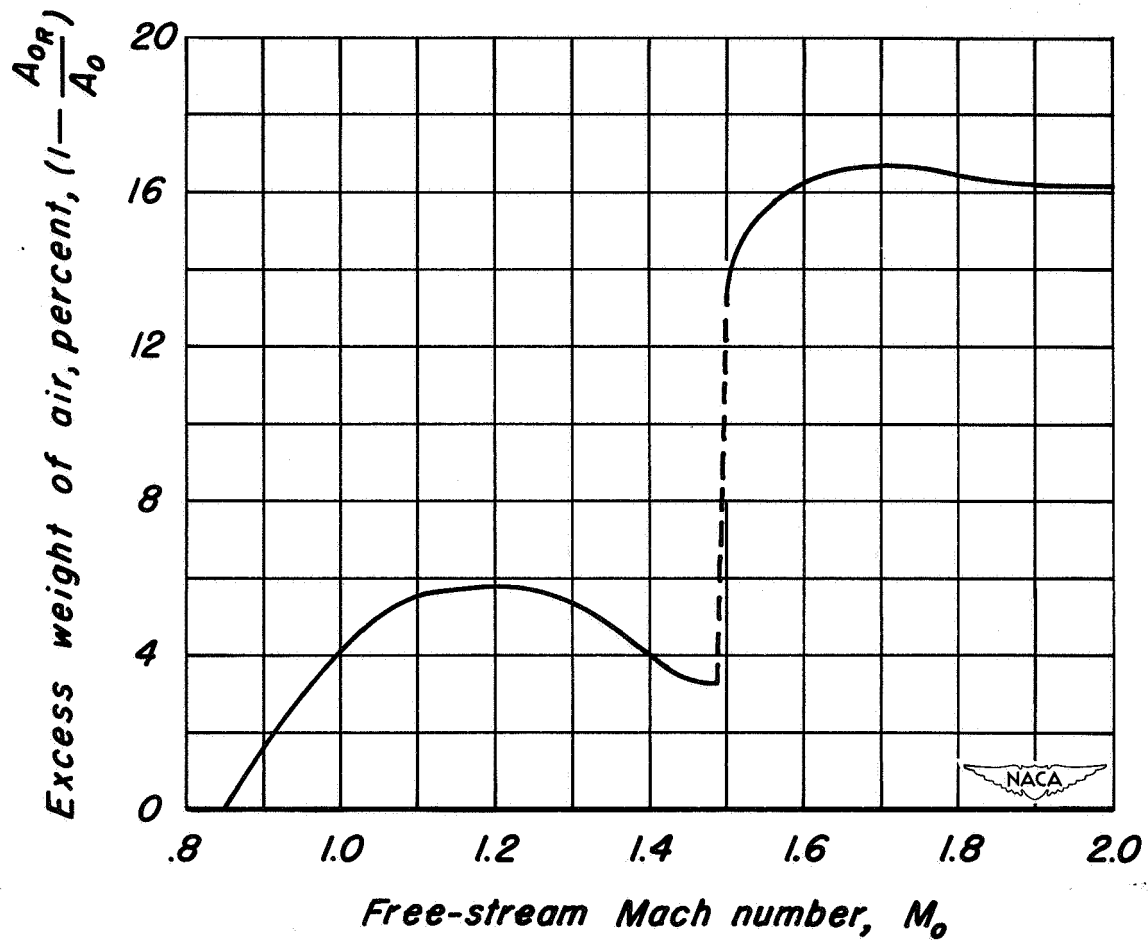
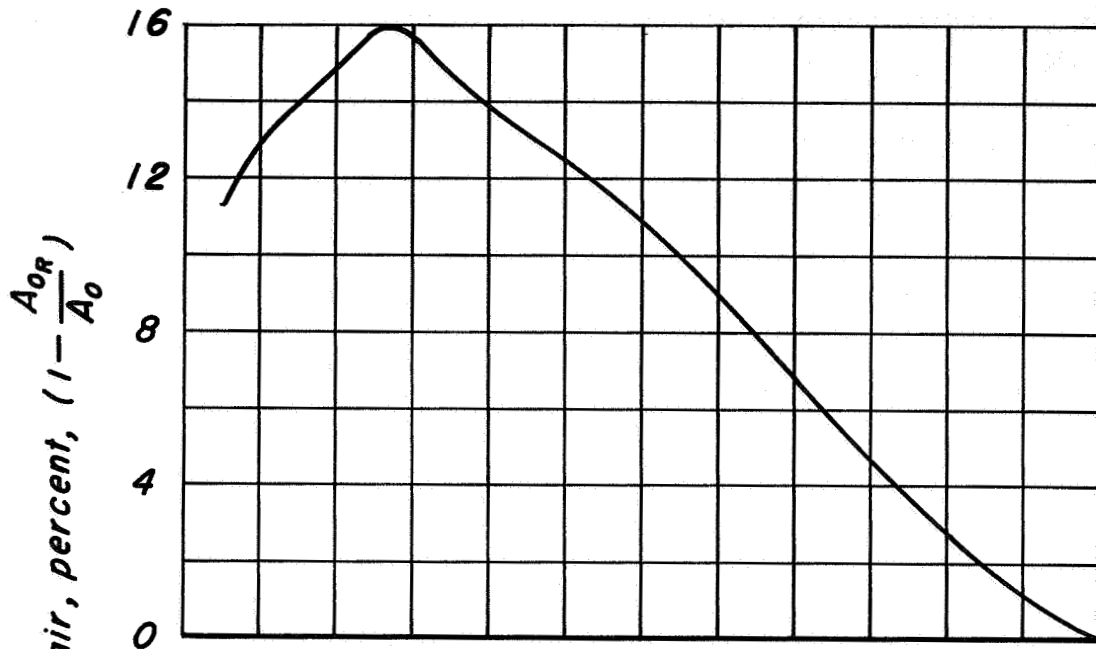


Figure 12.- The variation of the thrust-loss factor with free-stream Mach number for the pressure recovery for each inlet. Altitude, 35,332 feet.

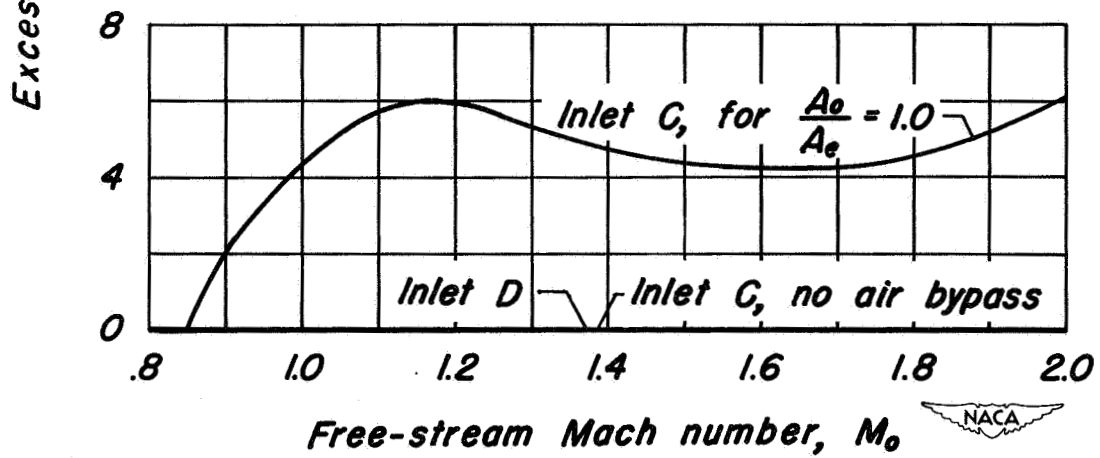


(a) Inlet A.

Figure 13.- The variation with free-stream Mach number of the percent of excess weight of air to be bypassed for each of the inlets. Altitude, 35,332 feet.



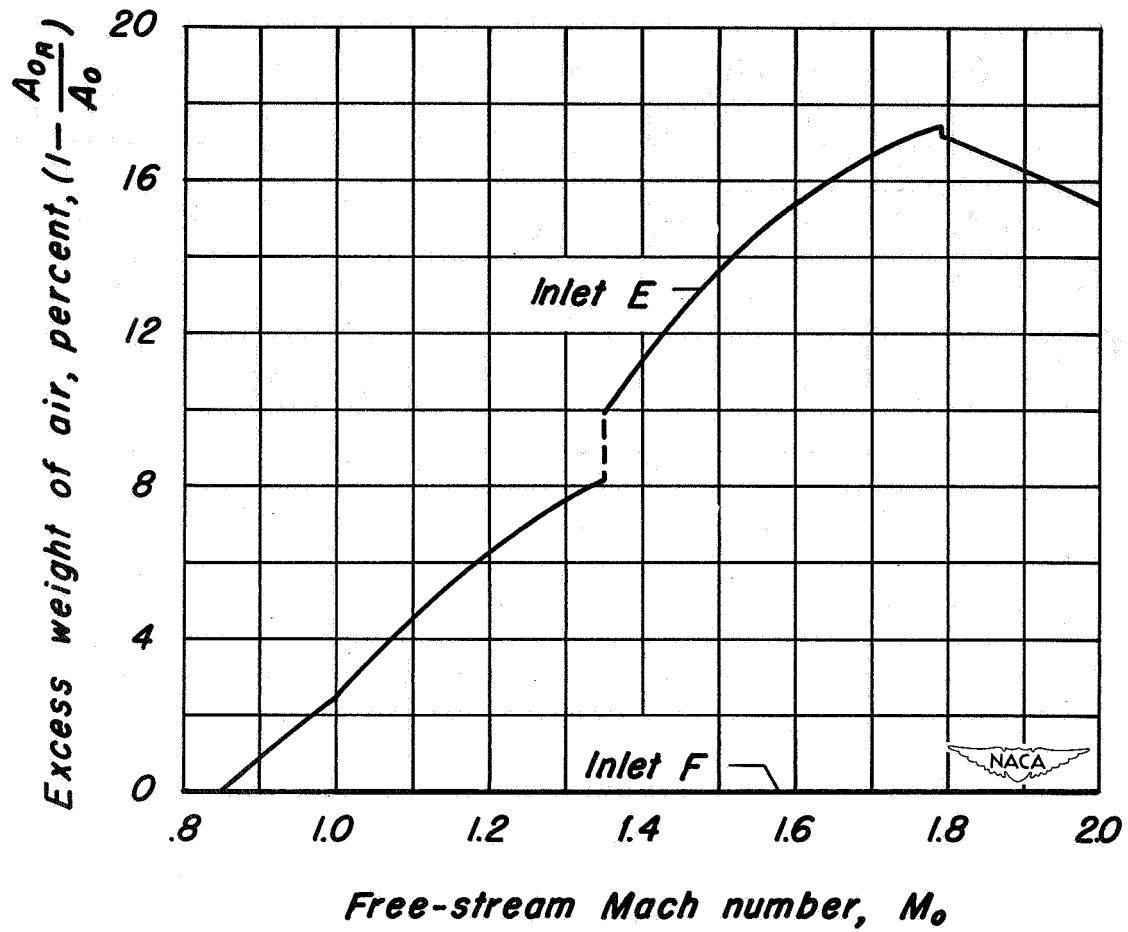
(b) Inlet B.



(c) Inlets C and D.

Figure 13.- Continued.

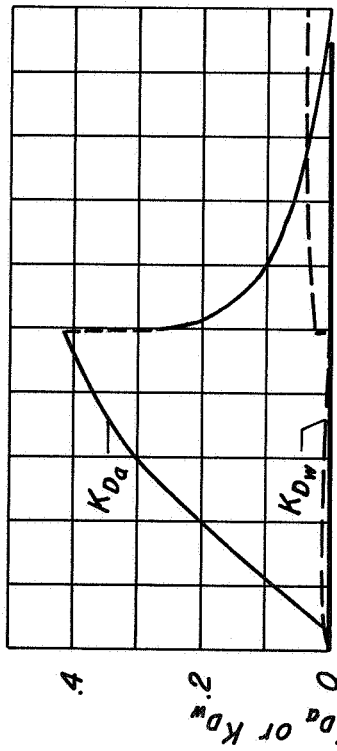




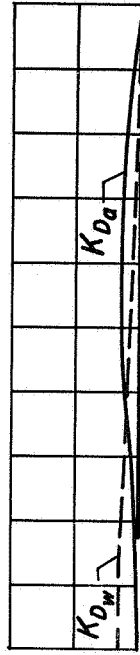
(d) Inlets E and F.

Figure 13.- Concluded.

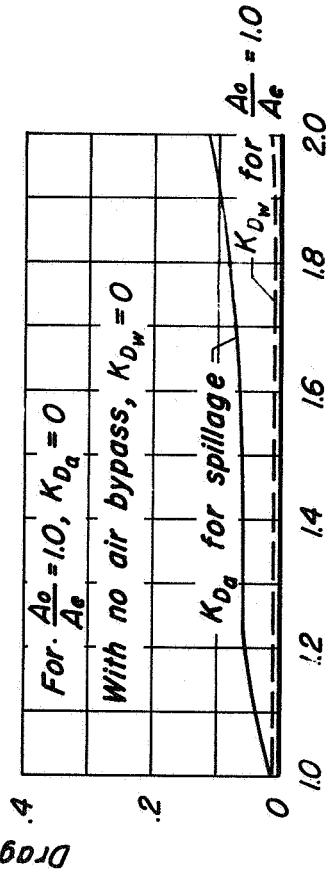
Note:- For inlets D and F both K_{D_a} and K_{D_w} equal zero.



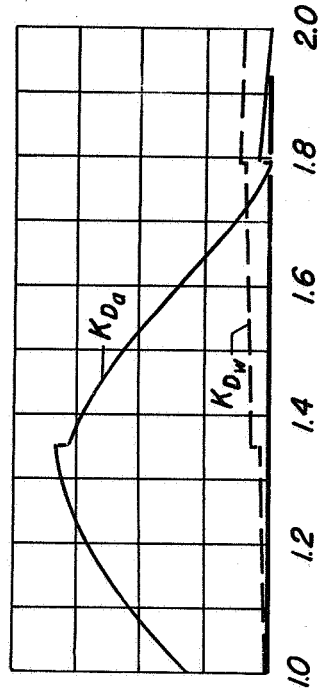
(a) Inlet A.



(b) Inlet B.



(c) Inlet C.



(d) Inlet E.

Figure 14.- The variation with free-stream Mach number of the additive-drag factor and the air-bypass-drag factor for each of the inlets. Altitude, 35,332 feet.

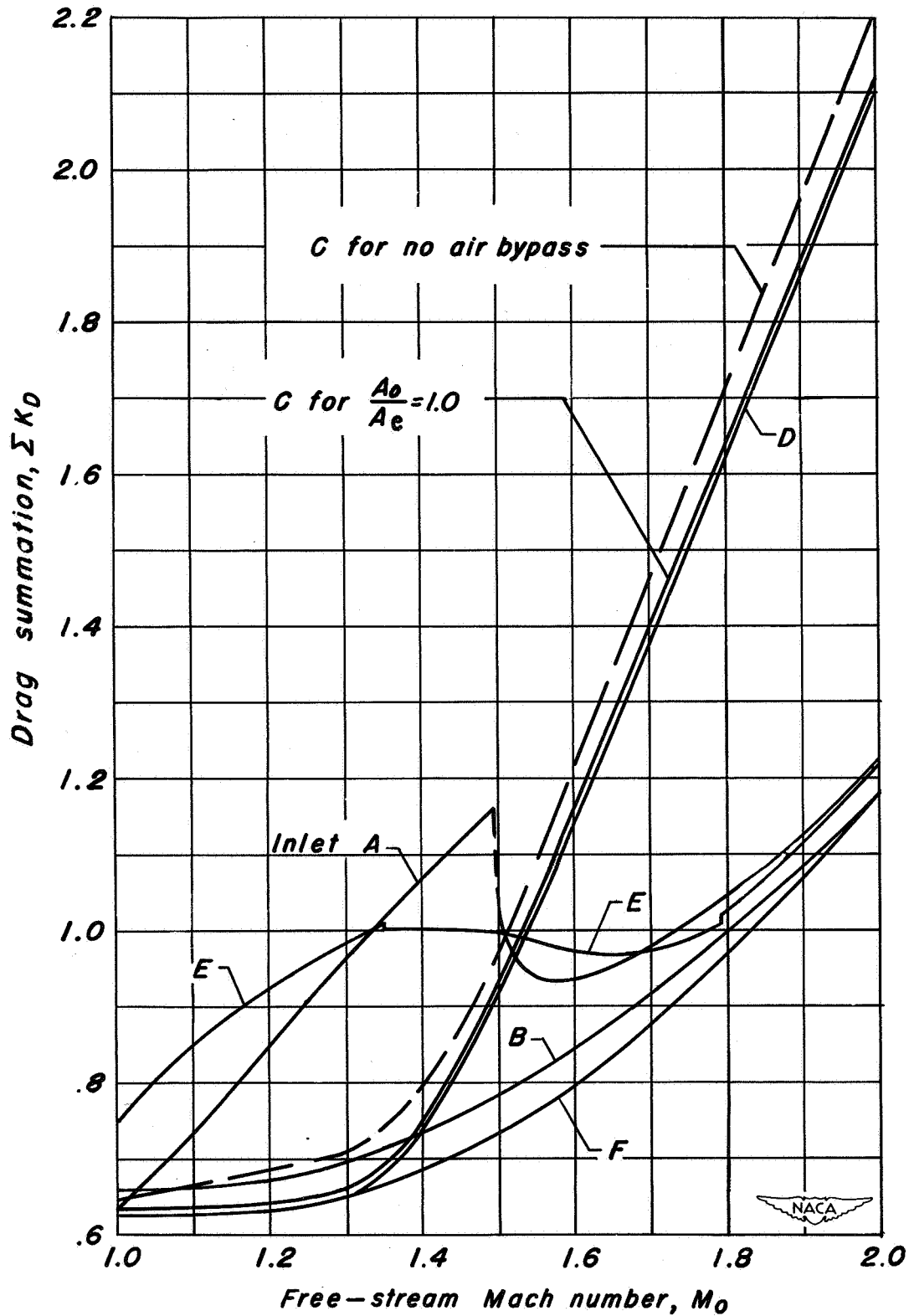


Figure 15.- The variation of the drag summation with free-stream Mach number for each of the inlets. Altitude, 35,332 feet.

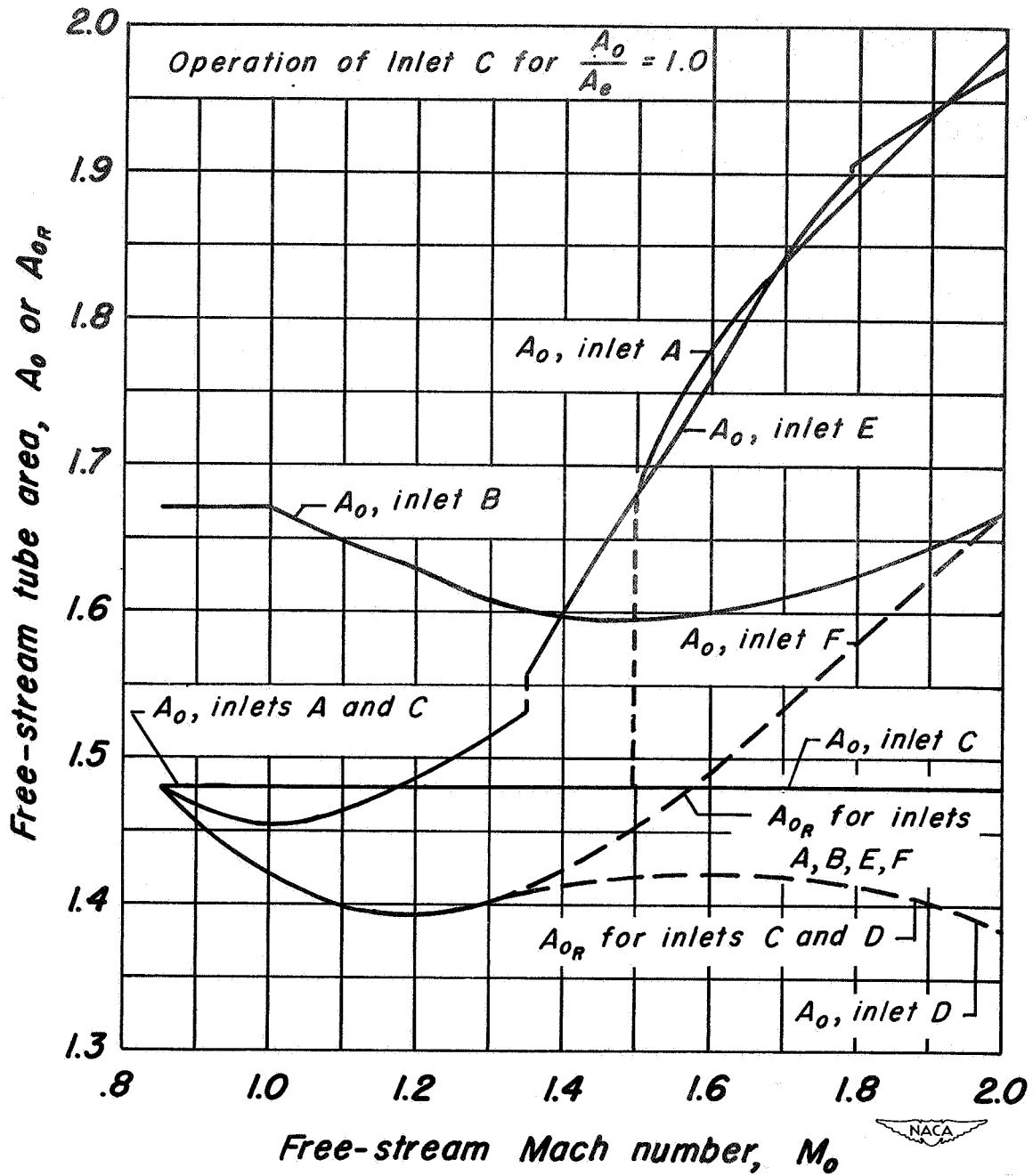
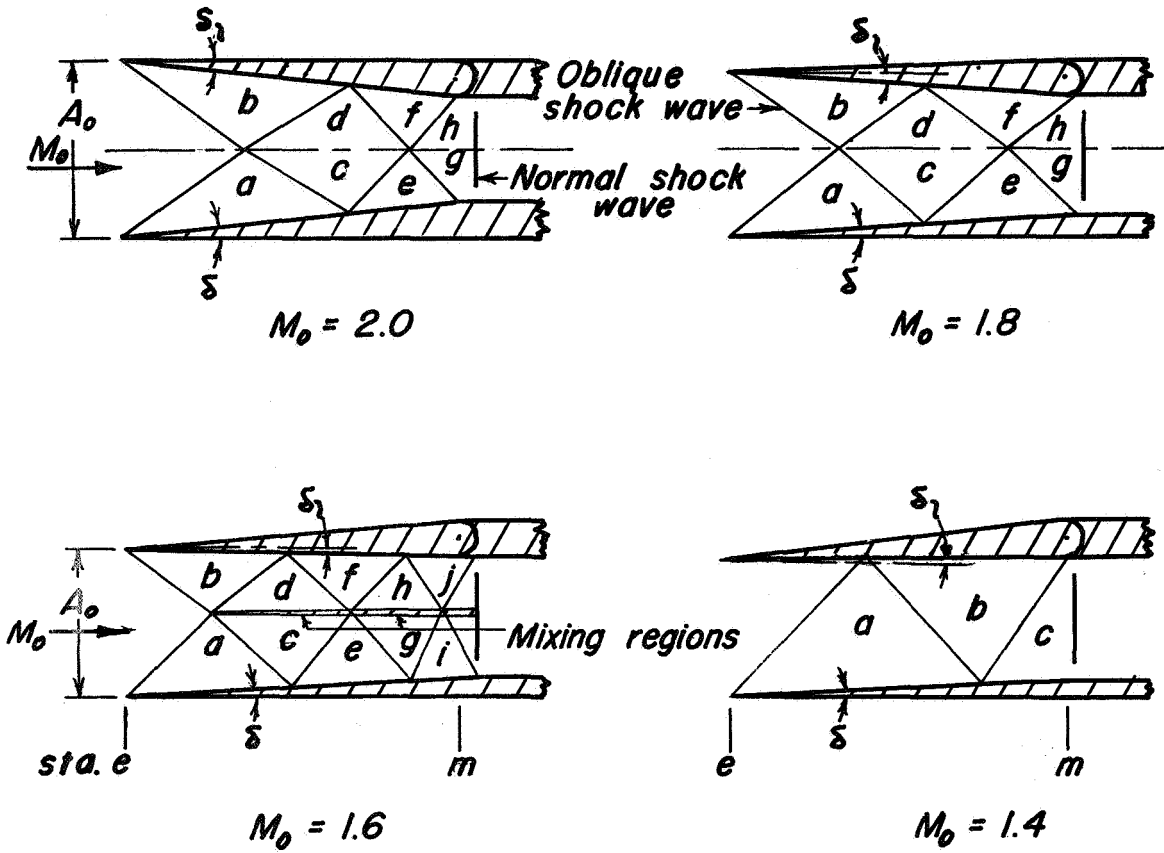


Figure 16.- Free-stream-tube areas; A_0 for each of the inlets and A_{0R} for the engine. Altitude, 35,332 feet.



Free-stream Mach number	$M_0=2.0$	$M_0=1.8$	$M_0=1.6$	$M_0=1.4$
H_g/H_0	0.950	0.972	0.978	0.979
$A_0=A_e=A_{0R}, ft^2$	1.926	1.788	1.627	1.517
δ, deg	6	3.68	3.29	(-)0.42
δ_l, deg	6	3.68	1.31	2.0
A_0/A_m	1.644	1.358	1.220	1.071
H_m/H_0	.985	.979	.993	.998



Figure 17.- Some geometric features and aerodynamic characteristics for inlet F.